Original research

Gut microbiota influence anastomotic healing in colorectal cancer surgery through modulation of mucosal proinflammatory cytokines

Roy Hajjar ,[1,2,3,4] Emmanuel Gonzalez,[5,6] Gabriela Fragoso,[1,4] Manon Oliero,[1,4] Ahmed Amine Alaoui,[1,2,3,4] Annie Calvé,[1,4] Hervé Vennin Rendos,[1,4] Souad Djediai,[7] Thibault Cuisiniere,[1,4] Patrick Laplante,[4,8] Claire Gerkins,[1,4] Ayodeji Samuel Ajayi,[1,4] Khoudia Diop,[4,9] Nassima Taleb,[2] Sophie Thérien,[2] Frédéricke Schampaert,[2] Hefzi Alratrout,[10] François Dagbert,[2,11] Rasmy Loungnarath,[2,11] Herawaty Sebajang,[2,11] Frank Schwenter,[2,11] Ramses Wassef,[2,11] Richard Ratelle,[2,11] Eric Debroux,[2,11] Jean-François Cailhier,[4,12,13] Bertrand Routy,[4,9,14] Borhane Annabi,[7] Nicholas J B Brereton ,[15,16] Carole Richard,[2,11] Manuela M Santos [1,4,12]

► Additional supplemental material is published online only. To view, please visit the journal online (http://dx.doi.org/10.1136/gutjnl-2022-328389).

For numbered affiliations see end of article.

Correspondence to
Dr Manuela M Santos, Nutrition and Microbiome Laboratory, Centre de recherche du Centre Hospitalier de l'Universite de Montreal (CRCHUM), Montréal H2X 0A9, Québec, Canada; manuela.santos@umontreal.ca

Received 1 August 2022
Accepted 8 December 2022

To cite: Hajjar R, Gonzalez E, Fragoso G, *et al*. *Gut* Epub ahead of print: [*please include* Day Month Year]. doi:10.1136/gutjnl-2022-328389

ABSTRACT

Objective Colorectal cancer (CRC) is the third most diagnosed cancer, and requires surgical resection and reconnection, or anastomosis, of the remaining bowel to re-establish intestinal continuity. Anastomotic leak (AL) is a major complication that increases mortality and cancer recurrence. Our objective is to assess the causal role of gut microbiota in anastomotic healing.

Design The causal role of gut microbiota was assessed in a murine AL model receiving faecal microbiota transplantation (FMT) from patients with CRC collected before surgery and who later developed or not, AL. Anastomotic healing and gut barrier integrity were assessed after surgery. Bacterial candidates implicated in anastomotic healing were identified using 16S rRNA gene sequencing and were isolated from faecal samples to be tested both *in vitro* and *in vivo*.

Results Mice receiving FMT from patients that developed AL displayed poor anastomotic healing. Profiling of gut microbiota of patients and mice after FMT revealed correlations between healing parameters and the relative abundance of *Alistipes onderdonkii* and *Parabacteroides goldsteinii*. Oral supplementation with *A. onderdonkii* resulted in a higher rate of leaks in mice, while gavage with *P. goldsteinii* improved healing by exerting an anti-inflammatory effect. Patients with AL and mice receiving FMT from AL patients presented upregulation of mucosal MIP-1α, MIP-2, MCP-1 and IL-17A/F before surgery. Retrospective analysis revealed that patients with AL present higher circulating neutrophil and monocyte counts before surgery.

Conclusion Gut microbiota plays an important role in surgical colonic healing in patients with CRC. The impact of these findings may extend to a vast array of invasive gastrointestinal procedures.

WHAT IS ALREADY KNOWN ON THIS TOPIC

⇒ Gut microbiota is hypothesised to play a role in the pathophysiology of anastomotic leak (AL).
⇒ The relation between gut microbiota and anastomotic healing is mainly based on correlational associations.

WHAT THIS STUDY ADDS

⇒ This is the first solid demonstration of a causal role of preoperative gut microbiota in the pathogenesis of AL in patients with colorectal cancer (CRC).
⇒ Gut microbiota influences local wound inflammation and subsequent repair by modulating the basal levels of mucosal cytokines.
⇒ Parabacteroides goldsteinii exerts locally an anti-inflammatory effect and improves the restoration of the gut barrier and wound healing.

HOW THIS STUDY MIGHT AFFECT RESEARCH, PRACTICE OR POLICY

⇒ Low-grade, subclinical intestinal inflammation may be assessed before surgery using sensitive inflammatory markers to identify patients at risk of developing AL.
⇒ P. goldsteinii represents a potential probiotic that may be assessed in early-phase clinical studies to improve postoperative recovery in patients with CRC at risk of developing AL.
⇒ These findings may be relevant to other invasive gastrointestinal procedures where targeting gut microbiota could present new treatment approaches.

INTRODUCTION

Colorectal cancer (CRC) is the third most diagnosed cancer and third-leading cause of cancer-related deaths.[1] Most patients with CRC require a surgical resection of the colon or rectum, which is followed by a reconnection, or anastomosis, of the remaining bowel ends to re-establish gastrointestinal continuity. Poor anastomotic healing may lead to leakage of the intestinal content into the abdominal cavity,

a major complication termed 'anastomotic leak' (AL). AL, which may occur in up to 30% of patients, leads to increased morbidity and mortality after surgery, delays in postoperative oncological care and longer hospital stay.[2] In addition, compelling data indicate that poor surgical recovery and AL are associated with increased risk of local[3] and distant[4] CRC recurrence. Recurrence of the cancer occurs in up to 30% of patients with stages I–III disease and up to 65% of those with stage IV disease.[5] The leakage of intestinal content through a poorly restored gut barrier after surgery leads to severe sepsis and systemic inflammation, which are believed to promote the dissemination and invasiveness of residual cancer cells.[6] Improving anastomotic healing to prevent AL in CRC surgery, therefore, represents a major goal to avoid complications and improve cancer outcomes.

After completion of the colorectal anastomosis, tissue repair begins immediately. It involves the production of a fibrin/fibronectin matrix that temporarily seals and connects the two bowel ends, an inflammatory stage and a remodelling phase, during which the new epithelium is developed and the final scar tissue is formed.[7] Normal epithelial growth and development is influenced by gut microbiota,[8–10] a collection of microbes, mainly bacteria, that inhabit the gastrointestinal tract and with highest density in the colon.[11] Gut microbiota may be involved in the process of bowel repair after surgery by modulating fibrosis[12] and the inflammatory phase.[13]

In this study, we investigated the causative role of gut microbiota in the pathogenesis of AL in patients with CRC.

RESULTS

Gut microbiota influence surgical outcomes in mice

To assess the potential role of gut microbiota in anastomotic healing, we first depleted gut microbiota in specific pathogen-free (SPF) wild-type mice by administering a broad-spectrum antibiotic regimen in drinking water (figure 1A–C). Mice were then subjected to colonic surgery using a previously validated model of poor anastomotic healing (online supplemental figure 1).[14] At postoperative day (POD) 6, mice with depleted gut microbiota displayed improved macroscopic healing of the colonic anastomosis (figure 1A) and a higher concentration of extracellular matrix (ECM) components in the wound (figure 1B,C), specifically hydroxyproline and fibronectin as indicators of collagen content and anastomotic consistency, respectively.

The myeloid differentiation factor 88 (MyD88) signalling pathway plays a fundamental role in the crosstalk that occurs between the intestine and its resident microbiota.[15] To further substantiate a role for gut microbiota in AL, we assessed colonic surgical healing in mice lacking MyD88 (figure 1D–F). When subjected to surgery, MyD88$^{-/-}$ mice displayed enhanced anastomotic healing and collagenisation of the wound than wild-type (WT) mice (figure 1D,E), and lower bacterial translocation to the spleen (figure 1F), as measured by colony-forming units, further highlighting the fundamental role of gut microbiota in surgical healing of the colon.

To further establish the causal relationship between gut microbiota and anastomotic healing in CRC surgery, stool samples of 77 patients were collected before surgery. Of those, nine patients later experienced AL and were matched for age, sex and tumour location with nine patients who did not experience AL (non-AL vs AL) (online supplemental table 1), and preoperative stool samples were transferred into antibiotic-conditioned mice by faecal microbiota transplantation (FMT) (figure 2). Transplanted mice were then subjected to surgery. FMT from patients with AL induced poorer colonic healing (figure 2A), a lower concentration of ECM components (figure 2B,C) and a higher concentration of E-cadherin (figure 2D), indicative of decreased cell migration capacity at the wound edges.[16] Lower concentrations

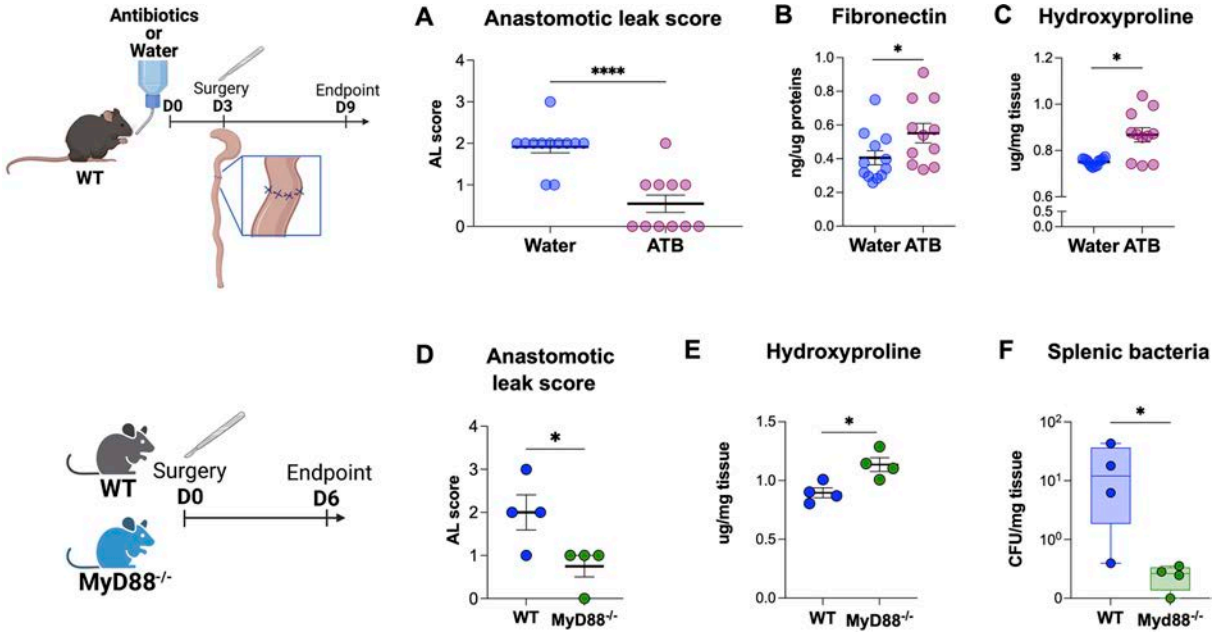

Figure 1 Anastomotic leak (AL) is modulated by gut microbiota in mice. (A–C) Mice received a combination of ampicillin, streptomycin and colistin (ATB) in drinking water or sterile water as a control and were subjected to colonic surgery. (A) Anastomotic leak (AL) score, (B) fibronectin and (C) hydroxyproline concentration at the anastomotic site. N=11–12 mice per group; each symbol represents one mouse with bars showing means±SEM; two-tailed Student's t-test. (D–F) SPF MyD88$^{-/-}$ and wild-type mice were subjected to colonic surgery and sacrificed 6 days later. (D) AL score and (E) hydroxyproline concentration at the anastomotic wound. N=4 per group, each symbol represents one mouse with bars showing means±SEM. Two-tailed Student's t-test. (F) splenic bacteria. N=4 per group, Mann-Whitney U test; data are represented as boxplots. *p<0.05, ****p<0.0001.

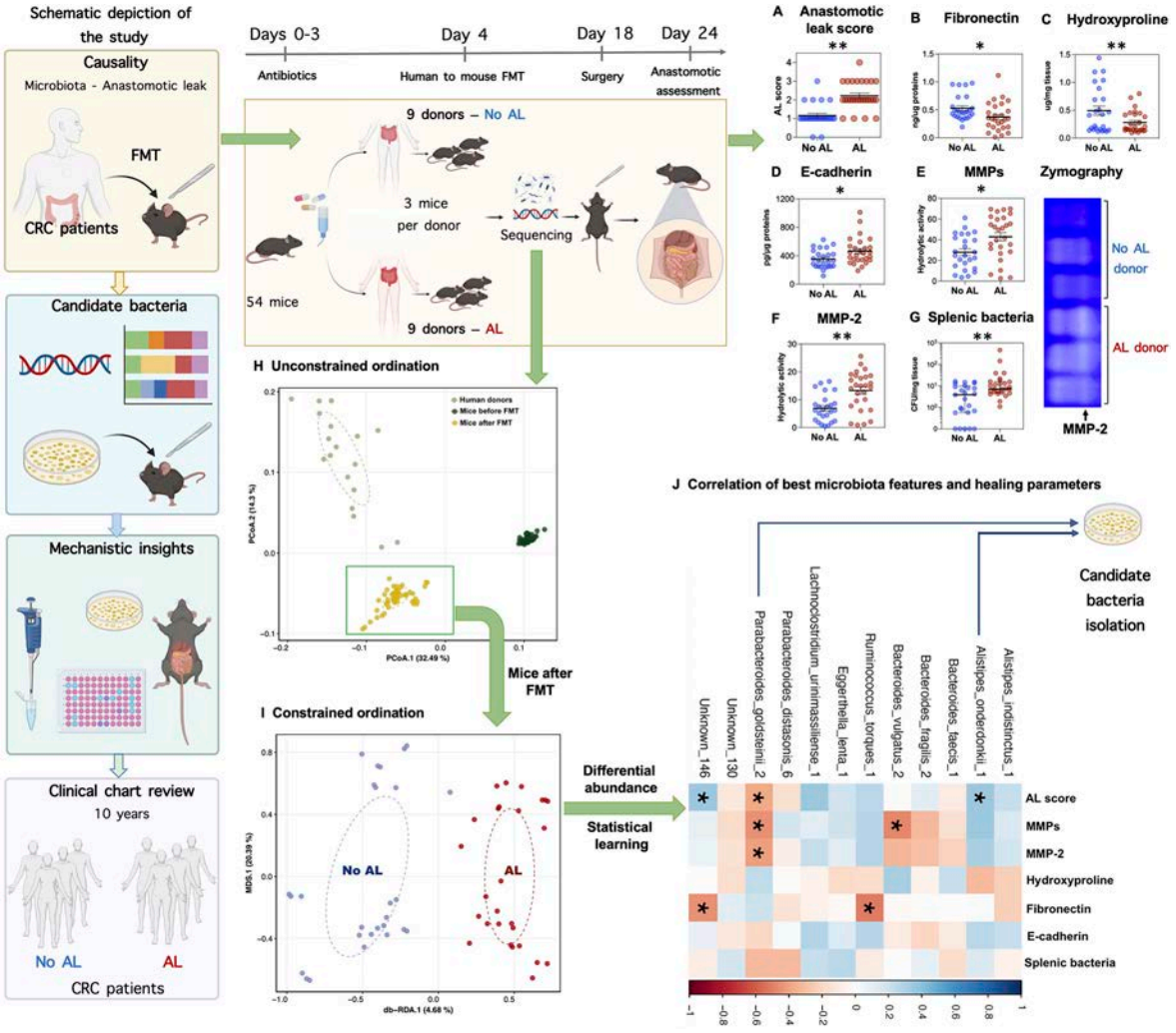

Figure 2 Gutmicrobiota influence colonic surgical healing in mice. The left panel depicts the structure of the study. (A–G) mice received faecal microbiota transplantation (FMT) from patients with colorectal cancer (CRC) without and with anastomotic leak (No AL and AL) before undergoing colonic surgery and were sacrificed 6 days later. (A) AL score, (B) fibronectin, (C) hydroxyproline and (D) E-cadherin concentration at the anastomotic wound. (E) Total MMPs and (F) MMP-2 activity as assessed by gelatin zymography. (G) splenic bacteria assessed by colony-forming units (CFU) counting. each symbol represents one mouse (N=25–27/group; 2–3 mice per donor, 9 donors per group); bars are means±SEM. P values were obtained using the generalised estimating equations to correct for covariance structure of mice from a same donor, *p<0.05, **p<0.01. (H) Principal coordinate analysis and (I) distance-based redundancy analysis of gut microbiota in faecal samples. (J) correlation matrix of bes AL predictive microbiota features in both mice and donors and healing parameters (Spearman correlation, *false discovery rate-adjusted (p<0.1).

of fibronectin and hydroxyproline were associated with higher collagen degradation involving mostly matrix metalloproteinase-2 (MMP-2; figure 2E,F). Lastly, FMT from donors with AL led to increased bacterial load in the spleen suggesting translocation from a weakened gut barrier (figure 2G).

To identify bacterial candidates implicated in anastomotic healing, microbial communities from stool samples of mice receiving FMT from patients with CRC with and without AL were assessed using 16S rRNA gene sequencing, and the ANCHOR pipeline[17] was used to process amplicon sequences and infer exact sequence variants (ESVs) (online supplemental figure 2A). Unconstrained principal coordinate analysis showed significant differences (p<0.001) between microbial communities in samples from mice before FMT, mice after FMT and human donors. The first axis (explaining 32.49% of total variance) separated samples into two distinct clusters, one consisting of mice samples before FMT and a second consisting of both transplanted mice and donor samples, which separated along the second axis (explaining 14.3% of total variance) (figure 2H). While alpha-diversity indexes did not differ between groups of mice before or after surgery (online supplemental figure 2B), (online supplemental table 2), significant differences in the bacterial communities of mice after FMT from non-AL and AL donors were observed using constrained beta-diversity analysis (distance-based redundancy analysis; p=0.004; figure 2I), suggesting different microbiota compositions in these two groups. Differential abundance analysis was performed between the non-AL and AL groups after FMT (FDR <0.05) (online supplemental figure 2C). Among the significantly differentially abundant ESVs, 28 could be putatively annotated at various taxonomic levels, including 24 species and 4 genera, 13 of which were higher in the non-AL group and 15 higher in the AL group.

Taken together, these data provide convincing evidence that preoperative gut microbiota composition influences postoperative healing.

Alistipes onderdonkii and *Parabacteroides goldsteinii* modulate anastomotic healing in mice

Next, to validate the hypotheses that non-AL versus AL donor associated microbiota were passed on to mice and persisted after FMT, and that non-AL versus AL microbiome significant differences in mice are related to those in humans, a statistical learning algorithm was run involving differentially abundant ESVs in two successive steps (online supplemental figure 3). Twelve ESVs were found to predict with high accuracy the leak status in both mice and patients (figure 2J, online supplemental figure 3).

An ESV annotated as *Alistipes onderdonkii* was significantly associated with higher AL score (figure 2J, online supplemental figure 2C) and its previous isolation from abdominal abscesses suggests a pathogenic potential.[18] We first confirmed that patients with AL and mice receiving their microbiota presented a higher abundance of *A. onderdonkii* compared with non-AL patients and mice using quantitative PCR (qPCR) (online supplemental figure 4A,B and online supplemental table 3). To explore the role of *A. onderdonkii* in AL, SPF wild-type mice that do not harbour this species in their gut (online supplemental figure 4C) received an oral gavage of an *A. onderdonkii* strain kh33 isolated from a human stool sample (CRCHUM collection), and sharing 100% sequence identity of the variable V5–V6 region of a 16S rRNA gene with *A. onderdonkii*'s ESV (online supplemental figure 5), and were then subjected to colonic surgery (figure 3). On POD 6, mice receiving the *A. onderdonkii* kh33 displayed a higher rate of leaks and abscesses when compared with mice receiving saline as a control (figure 3A). In addition, they displayed lower hydroxyproline concentration at the anastomotic site and increased bacterial translocation to the spleen (figure 3B,C). Next, we tested another member of the same genus, *Alistipes indistinctus*, that was also found to be significantly more abundant in mice receiving FMT from donors with AL (online supplemental figure 4E). However, unlike *A. onderdonkii,* the administration of *A. indistinctus* strain kh34 (CRCHUM collection) did not influence clinical outcomes (online supplemental figure 4G).

A second ESV, annotated as *Parabacteroides goldsteinii* 2, presented an abundance profile that correlated with improved AL scores and lower MMPs levels (figure 2J, (online supplemental figure 2C), suggesting a potential protective effect. Using qPCR (online supplemental table 3), we confirmed that patients without AL, and their respective transplanted mice, presented increased levels of *P. goldsteinii* 2 (online supplemental figure 6A,B). We isolated *P. goldsteinii* strain kh35 from a human stool sample (CRCHUM collection), which shared 100% sequence identity of the variable V5–V6 region of a 16S rRNA gene with *P. goldsteinii* 2 (online supplemental figure 7) and was undetectable in naïve mice (online supplemental figure 6C). When *P. goldsteinii* kh35 was administered to mice before subjecting them to colonic surgery, the AL score improved significantly (figure 3D). In addition, ECM components were enhanced while MMP-2 activity and splenic bacterial load were reduced (figure 3E,F, online supplemental figure 6D,E). To further confirm the beneficial effect of *P. goldsteinii* kh35 in improving gut healing after surgery, antibiotic-conditioned mice were colonised with microbiota from patients with AL and then received supplementation with *P. goldsteinii* kh35 or saline twice before surgery (figure 3, online supplemental figure 6F–H). Mice receiving *P. goldsteinii* kh35 had an improved leak score (figure 3G), greater postoperative weight recovery (online supplemental figure 6G), higher hydroxyproline and fibronectin concentration in the wound (figure 3H, online supplemental figure 6H) and lower splenic bacterial load (figure 3I). Finally, germ-free mice supplemented with *P. goldsteinii* kh35 showed an improved surgical recovery similar to that seen in germ-free mice that received FMT from healthy donors (online supplemental figure 8). Germ-free mice are known to have impaired gut physiology and repair capacity,[19 20] and this was recapitulated in our surgical model where untreated germ-free mice displayed poor colonic healing. These results suggest that *P. goldsteinii* kh35 improves surgical healing, strengthens the wound matrix, and reinforces the gut barrier.

Oral gavage with supernatants obtained from *A. onderdonkii* kh33 and *P. goldsteinii* kh35 cultures replicated the effects seen with live bacteria supplementation in mice subjected to surgery (online supplemental figure 9), indicating that factors produced and released by these species can affect the outcomes of anastomotic healing. Finally, *P. goldsteinii* kh35 and *A. onderdonkii* kh33 were found to be present in colonic mucosal samples collected during surgery before the completion of the anastomosis (online supplemental figure 10A), as well as in mucosal anastomotic samples taken from mice after surgery, where the levels of *P. goldsteinii* two were lower, while those of *A. onderdonkii* were higher in mice with FMT from donors with AL compared with mice with FMT from donors that healed uneventfully (online supplemental figure 10B). These data indicate that *P. goldsteinii* and *A. onderdonkii* adhere to the colonic mucosa and are not affected by prophylactic antibiotics and mechanical bowel preparation that patients receive before surgery.

P. goldsteinii reduces the release of inflammatory cytokines by inhibiting the MyD88/NF-κB signalling pathway

Previous studies reported that another *P. goldsteinii* strain, which shares 100% sequence identity of the variable V5–V6 region of the 16S rRNA gene with *P. goldsteinii* 1 in our study, presented anti-inflammatory properties in a murine lung inflammation model.[21] We reasoned that *P. goldsteinii* kh35 may produce and release anti-inflammatory molecules. Therefore, we prepared cell-free supernatants of *P. goldsteinii* kh35 cultures grown in RPMI medium and investigated its ability to affect the activation of the MyD88-dependent signalling pathway. Using THP-1 monocytic cells exposed to *Escherichia coli* lipopolysaccharide, we found that *P. goldsteinii* kh35 supernatant reduced the expression of MyD88, the activation of the nuclear factor-kappa B (NF-κB) and subsequent tumour necrosis factor (TNF)-α mRNA expression (figure 3J–M).[22] In contrast, supernatant from *A. onderdonkii* kh33 strongly activated NF-κB in THP-1 cells (online supplemental figure 11). These data suggest that mechanistically, *P. goldsteinii* kh35 improves anastomotic healing through an anti-inflammatory effect by suppressing the MyD88/NF-κB signalling pathway.

Upregulation of mucosal inflammatory cytokines in patients with AL and mice receiving FMT from patients with AL before surgery

Given the importance of microbiota-driven local inflammation in postoperative gut healing,[23] we questioned whether patients with AL could have presented subclinical inflammation in the gut before AL occurrence, which is not routinely assessed in the standard preoperative evaluation. We found that among a multiplex panel of nine cytokines tested in mucosal samples, four differentially expressed cytokines were transferable by FMT into mice (figure 4 and online supplemental figure 12). AL patients (figure 4A), and their respective transplanted mice (figure 4B), harboured higher basal levels of pro-inflammatory cytokines, namely macrophage inflammatory protein 1 alpha

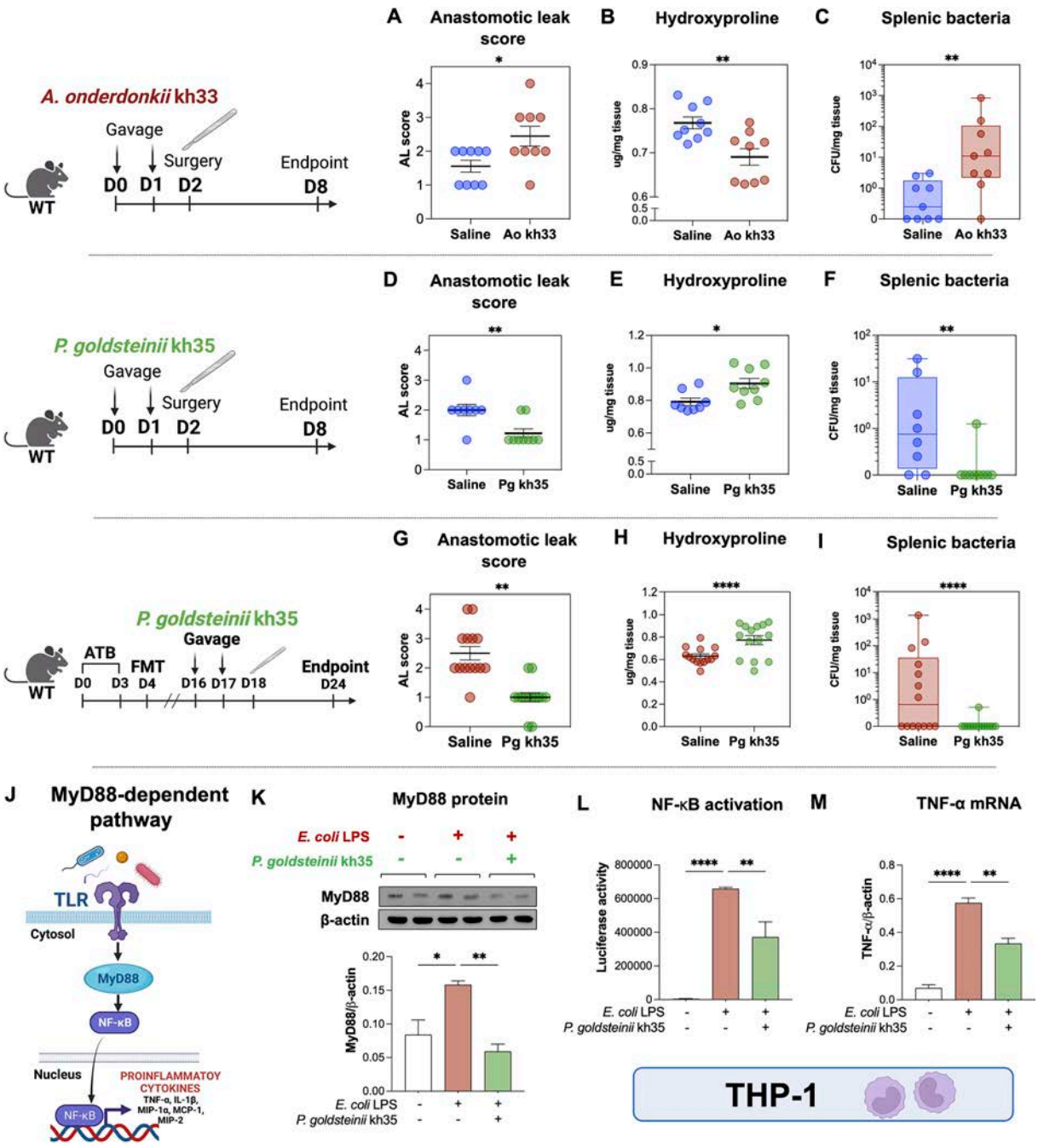

Figure 3 *Alistipes onderdonkii* kh33 and *Parabacteroides goldsteinii* kh35 affect surgical colonic healing in mice. (A–F) Specific pathogen-free (SPF) mice received daily gavage of saline, *A. onderdonkii* kh33 (Ao kh33), or *P. goldsteinii* kh35 (Pg kh35) before undergoing colonic surgery. (A and D) Anastomotic leak (AL) score and (B and E) hydroxyproline concentration at the anastomotic wound (N=8–9 mice per group; each symbol represents one mouse with bars showing means±SEM; two-tailed Student's t-test). (C and F) Splenic bacteria (boxplots; Mann-Whitney U test). (G–I) Mice received antibiotics (ATB) before FMT from patients ith CRC with AL and then received gavage with *P. goldsteinii* kh35 before undergoing colonic surgery. (G) AL score, (H) hydroxyproline concentration and (I) splenic bacteria (N=14 per group; 2–3 mice per donor; 5 donors per group). (J) Schematic depiction of the MyD88-dependent pathway. (K–M) THP-1 cells were treated with *Escherichia coli* LPS and were incubated with *P. goldsteinii* kh35 supernatant. (K) MyD88 expression assessed by western blot (one representative blot is shown and the graph below represents quantification of N=3 experiments). (L) NF-$_{\kappa}$B activation (luciferase activity) and (M) TNF-α mRNA expression (N=3–4 experiments; bars represent means±SEM; ANOVA with Tukey's *post hoc* test). *p<0.05, **p<0.01, ****p<0.0001. ANOVA, analysis of variance; CRC, colorectal cancer.

and 2 (MIP-1α and MIP-2), monocyte chemoattractant protein 1 (MCP-1), and interleukin-17A/F (IL-17A/F).

Next, we tested whether *A. onderdonkii* kh33 and *P. goldsteinii* kh35 could affect the production of the identified cytokines. We found that oral gavage with *A. onderdonkii* kh33, but not *A. indistinctus* kh34, increased faecal levels of MIP-1α, MIP-2 and IL-17A/F before surgery (online supplemental figure 13A,B). Conversely, oral *P. goldsteinii* kh35 inhibited the production of those three cytokines as well as MCP-1 levels, both in mice with native gut microbiota and mice that received FMT from AL donors (online supplemental figure 13C,D). To further confirm the relationship between the three chemokines and impaired

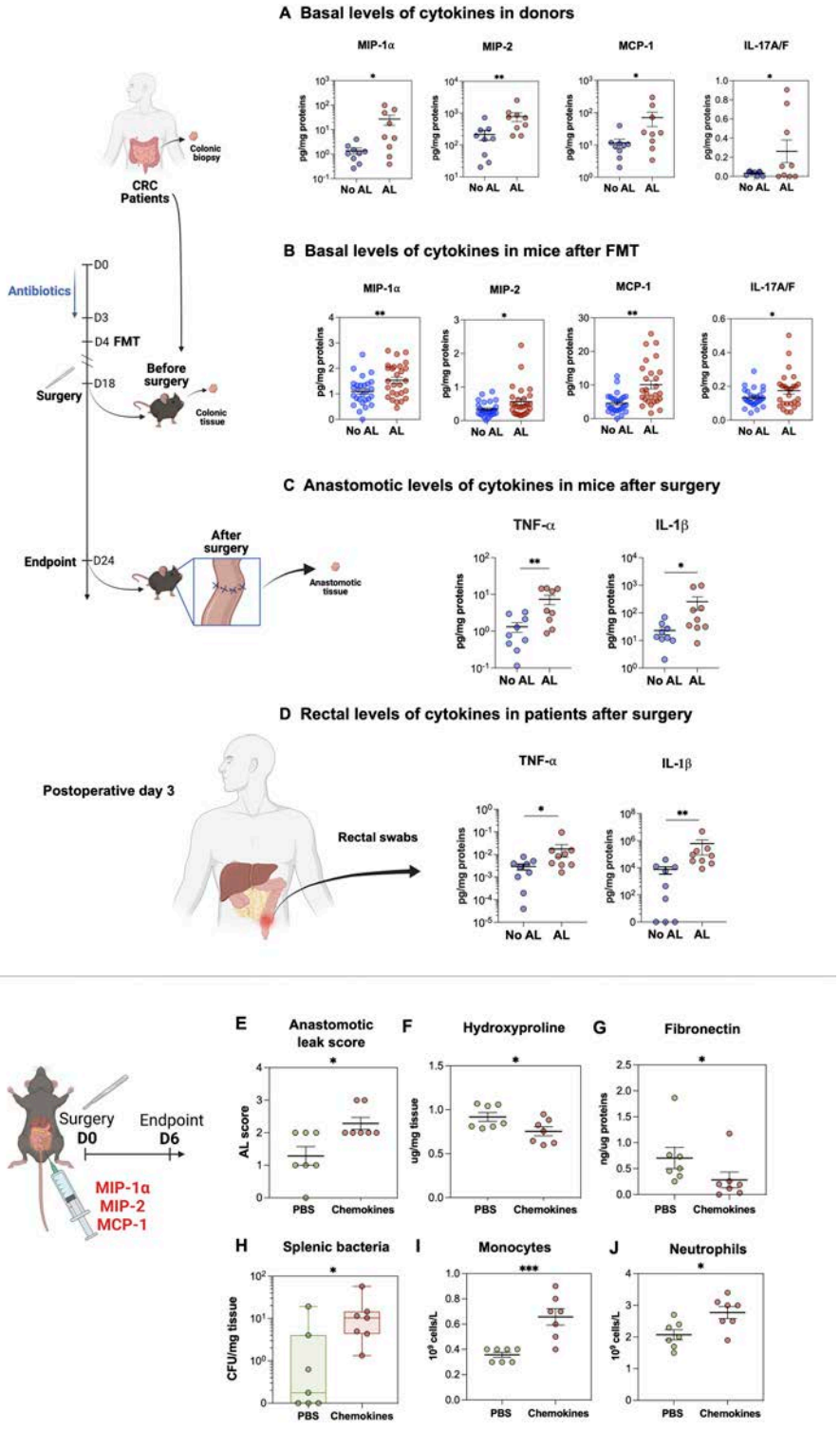

Figure 4 Enhanced preoperative mucosal cytokines levels result in heightened inflammation after surgery, and impair anastomotic healing in mice. (A and B) Mucosal biopsies were collected from patients at surgery, and from mice 2 weeks after receiving faecal microbiota transplantation (FMT) from patients with CRC without and with anastomotic leak (No AL and AL). (A) Basal levels of MIP-1α, MCP-1, MIP-2 and IL-17A/F in the colonic mucosa of patients with CRC (N=9 per group; each symbol represents one patient; two-tailed Student's t-test). (B) MIP-1α, MIP-2, MCP-1 and IL-17A/F levels were assessed in mice after FMT (N=27 mice per group; 3 mice per donor; 9 donors per group; GEE). (C and D) TNF-α and IL-1β levels in (C) anastomotic tissue collected from mice at the end of the experiment (each symbol represents pooled samples from 2 to 3 mice per donor for a total of 9 donors per group and (D) in rectal mucosal swabs collected from patients at postoperative day 3. (N=9 per group; each symbol represents one patient; two-tailed Student's t-test). (E–J) Mice received an intraperitoneal injection of recombinant MIP-1α, MCP-1 and MIP-2, or phosphate buffered saline (PBS) before surgery, and were then subjected to colonic surgery. (E) Anastomotic leak (AL) score, (F) hydroxyproline and (G) fibronectin concentration at the anastomotic wound. Two-tailed Student's t-test, bars represent means±SEM. (H) Splenic bacteria. Mann-Whitney U test; data are represented as boxplots. Circulating levels of (I) monocytes and (J) neutrophils at endpoint. Two-tailed Student's t-test. N=7 per group. *p<0.05, **p<0.01, ***p<0.001. AL, anastomotic leak; CRC, colorectal cancer.

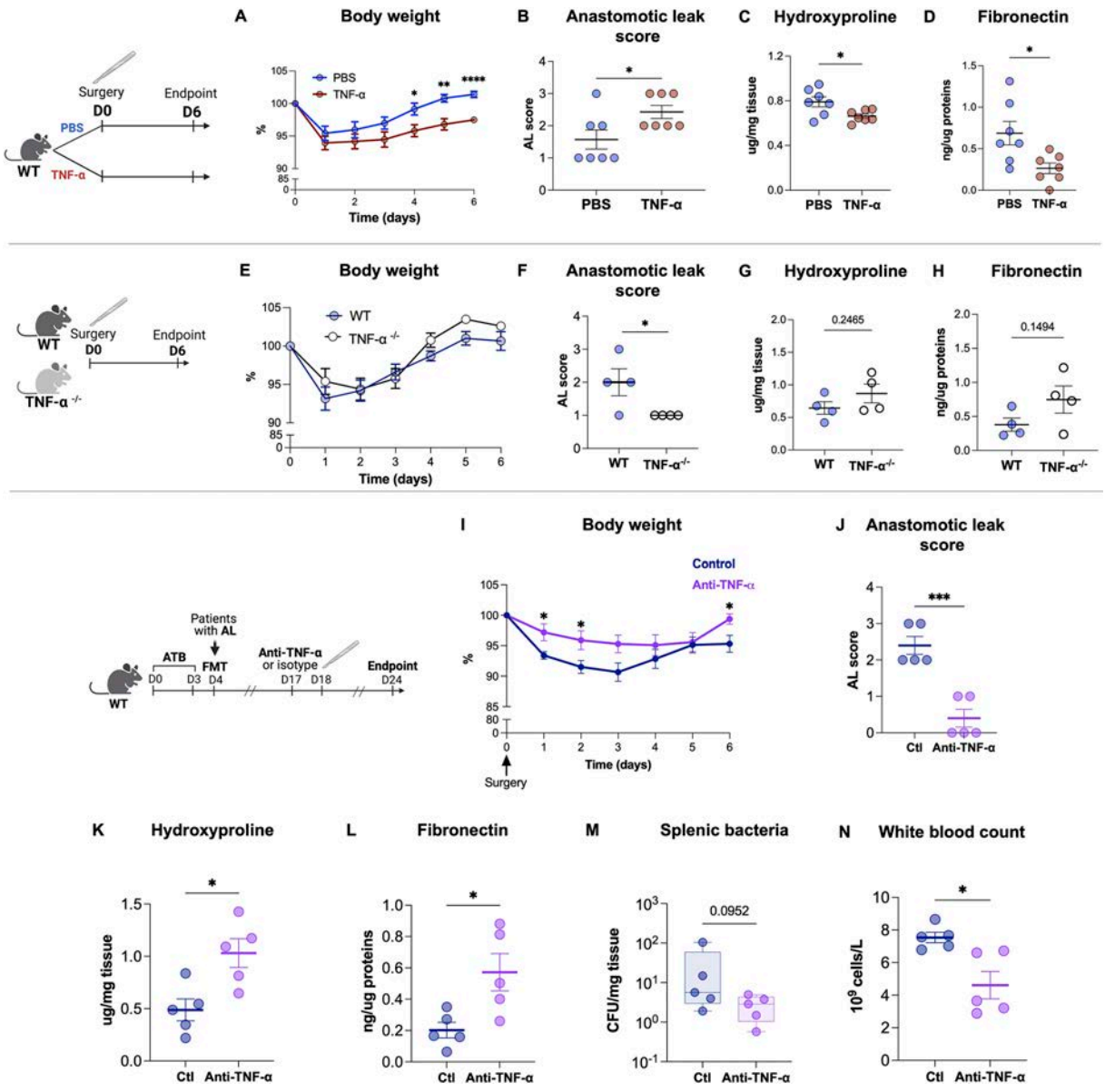

Figure 5 TNF-α influences anastomotic healing in mice undergoing colonic surgery. (A–D) SPF wild-type mice received, before surgery, an intraperitoneal injection of TNF-α, or PBS as control and were subjected to colonic surgery. (A) Body weight of mice after surgery. (B) Anastomotic leak (AL) score, (C) hydroxyproline and (D) fibronectin at the anastomotic wound. N=7 mice per group, each dot represents one mouse with bars showing means±SEM, two-tailed Student's t-test. (E–H) Wild-type and TNF-α$^{-/-}$ mice subjected to colonic surgery. (E) body weight, (F) anastomotic leak (AL) score, (G) hydroxyproline and (H) fibronectin concentration at the anastomotic wound (N=4 mice per group, each dot represents one mouse with bars showing means±SEM, two-tailed Student's t-test). (I–N) Mice received antibiotics (ATB) before FMT from patients with CRC with AL and were then injected with control isotype (Ctl) or TNF-α antibody. (I) body weight, (J) anastomotic leak (AL) score, (K) hydroxyproline and (L) fibronectin concentration at the anastomotic wound (N=5 mice per group, each dot represents one mouse with bars showing means±SEM, two-tailed Student's t-test). (M) Splenic bacteria. Boxplots, Mann-Whitney U test. (N) White cell count. Data are presented as means±SEM, two-tailed Student's t-test. *p<0.05, ***p<0.001.

healing, SPF wild-type mice received a cocktail of recombinant MIP-1α, MIP-2 and MCP-1 before being subjected to colonic surgery (figure 4E–J). Although not perfect, this treatment increases the levels of those cytokines in the peritoneal cavity before surgery, as an attempt to mimic enhanced preoperative levels found in AL patients. Treatment with the chemokines cocktail impaired anastomotic healing in mice, and increased circulating monocyte and neutrophil levels (figure 4E–J).

These results show that patients with AL present an upregulation of mucosal inflammatory cytokines before surgery and this profile can be transferred to mice via FMT. Elevated levels of the identified cytokines could be associated with poor wound repair after surgery, and their production is affected in opposite directions by *A. onderdonkii* kh33 and *P. goldsteinii* kh35.

Upregulation of mucosal inflammatory cytokines before surgery enhances inflammation after surgery

IL-17A has been shown to play a key role in the mobilisation of inflammatory monocytes producing TNF-α and IL-1β-secreting neutrophils.[24] In turn, high levels of TNF-α and IL-1β are hallmarks of chronically inflamed intestinal wounds failing to heal,[25 26]

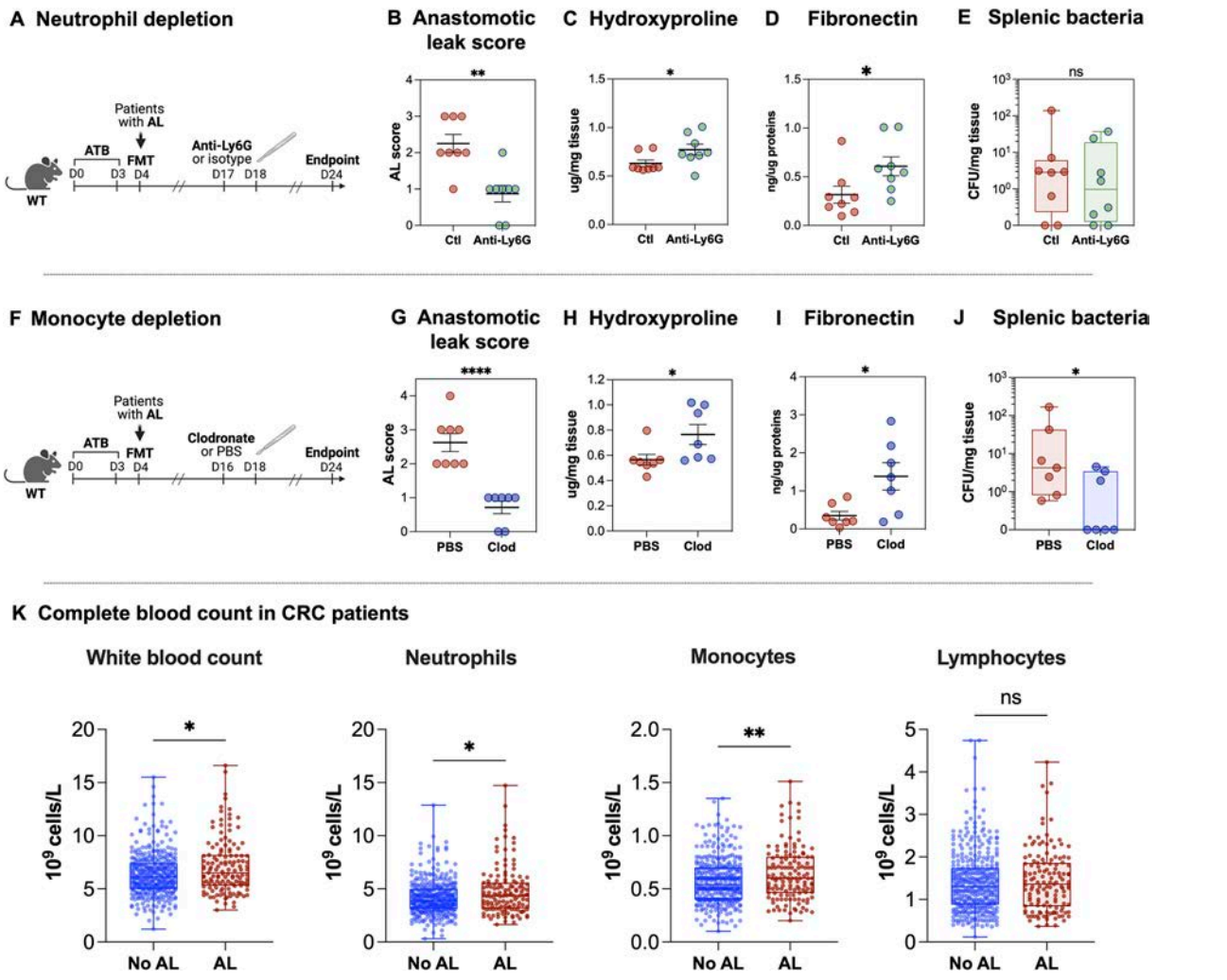

Figure 6 Higher preoperative circulating neutrophil and monocyte counts are associated with impaired anastomotic healing. Mice were colonised by faecal microbiota transplantation (FMT) from a pooled faecal sample of four donors with anastomotic leak (AL), and partial depletion of (A–E) neutrophils and (F–J) monocytes (A and F) was performed using anti-Ly6G antibody or clodronate liposomes respectively (N=7–8 per group). (B and G) AL score, (C and H) hydroxyproline and (D and I) fibronectin concentration in anastomotic wounds (bars represent means±SEM; two-tailed Student's t-test). (E and J) Splenic bacteria (boxplots, Mann-Whitney U test). (K) Preoperative white cell counts of patients experiencing AL from 2011 to 2021 (N=135) and of patients with uneventful recovery that were randomly selected (N=360 out of 1750). *p<0.05, **p<0.01, ****p<0.0001. NS, non-significant.

and may impair wound healing by activating matrix-degrading collagenases and inhibiting regeneration mechanisms.[27 28] In fact, in our cohort, patients who developed AL displayed significantly higher levels of TNF-α and IL-1β in rectal swabs collected at POD 3 compared with patients with uneventful healing (No AL; figure 4D). We, therefore, reasoned that low-grade inflammation present before surgery could potentiate inflammation after surgery. Indeed, mice receiving FMT from leaky donors had increased TNF-α and IL-1β at the anastomotic wound compared with FMT mice from non-AL patients (figure 4C). Furthermore, mice treated with TNF-α before surgery showed impaired anastomotic healing, while TNF-$\alpha^{-/-}$ mice and mice treated with anti-TNF-α antibodies after FMT from AL donors displayed improved healing (figure 5), further confirming the deleterious effect of pre-existing heightened inflammation on colonic anastomotic healing. As shown in online supplemental figure 14, TNF-α neutralisation did not affect the levels of *P. goldsteinii* and *A. onderdonkii* in faecal samples. Taken together, these results suggest that gut microbiota-driven low-grade inflammation present before surgery leads to enhanced inflammation after surgery, resulting in poor healing capacity.

Higher circulating levels of monocytes and neutrophils are associated with impaired anastomotic healing in patients with CRC

From a translational point of view, we next explored the relationship between neutrophils and monocytes blood counts and faecal inflammatory markers in patients with CRC, which could have a predictive value. We found that preoperative neutrophil and monocyte blood counts in the 18 donors inversely correlated with faecal *P. goldsteinii* 2 levels and were positively associated with the faecal inflammatory marker lipocalin-2, an antimicrobial peptide produced mainly by neutrophils, but not with calprotectin (online supplemental figure 15). Next, to further understand the role of neutrophils and monocytes in anastomotic healing, we tested whether their depletion would influence colonic healing in mice. Neutrophil or monocyte partial depletion in mice prior to surgery using anti-Ly6G antibodies and clodronate liposomes respectively (figure 6A and F, online supplemental figure 16) prevented abscesses and leaks and improved the recovery of the wound matrix (figure 6A–J),

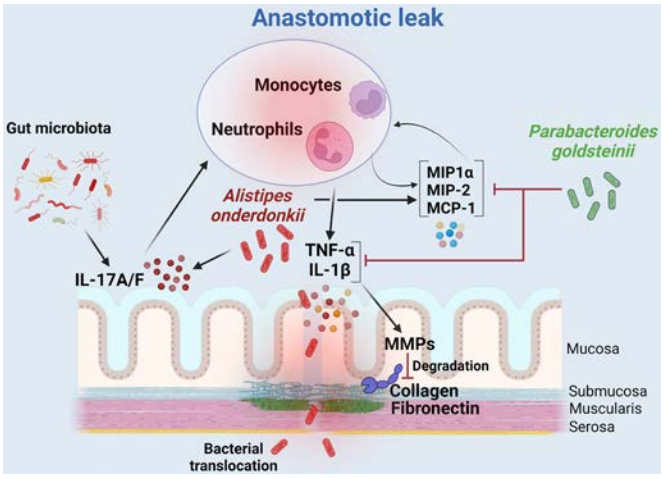

Figure 7 Graphical abstract of the study results.

underscoring the importance of the circulating levels of these cells before surgery. We next wondered whether preoperative levels of neutrophils and monocytes in the blood of patients with CRC could be associated with AL occurrence after surgery. Thus, the white cell count (WCC) of patients with CRC experiencing AL in our centre were compared with those of patients without AL (online supplemental table 4). Patients experiencing AL had significantly higher preoperative WCC, driven by elevated neutrophil and monocyte, but not lymphocyte counts (figure 6K). These results highlight the potential usage of biological markers before surgery to identify patients with CRC at risk of developing AL.

DISCUSSION

Our study provides evidence that microbiota-driven upregulation of proinflammatory cytokines in the colon before surgery influences anastomotic healing after surgery. We further identified two bacterial strains, *Alistipes onderdonkii* kh33 and *Parabacteroides goldsteinii* kh35, which modulate anastomotic healing namely by regulating the basal levels of proinflammatory cytokines in the gut (figure 7).

To the best of our knowledge, this study constitutes the first solid demonstration of a causal role of the preoperative gut microbiota in surgical healing in patients with CRC. Previous studies have assessed potential correlations between the composition of the gut microbiota and AL,[29 30] however, no direct causal relationship has been assessed using human FMT with preoperative faecal samples in animal surgical models. Our findings show that, beyond correlational comparisons, transferable preoperative bacterial species influence colonic healing in mice and AL. An additional important finding was that patients experiencing AL presented elevated mucosal proinflammatory cytokines already before surgery. This phenotype was transferrable from patients to mice by gut microbiota transplantation, indicating that upregulation of mucosal proinflammatory cytokines is dependent on gut microbiota composition. AL usually leads to significant local and systemic sepsis,[31] and we show that the postoperative inflammatory reaction was indeed exacerbated in AL patients, as evidenced by the higher levels of TNF-α and IL-β measured in rectal swabs obtained after surgery. Our finding is in agreement with recent findings showing that FMT in mice using postoperative stool samples from patients with AL induced poor anastomotic healing in rats.[32] Similar relationship between the presence of proinflammatory cytokines such as TNF-α, and deficient mucosal repair[25] have been reported in chronic inflammatory gut conditions, namely in inflammatory bowel disease.[33] In turn, IL-1β has been shown to contribute to a sustained inflammatory environment by inducing continuous accumulation of IL-17A,[26] which may lead to the establishment of a chronic wound that persists in the inflammatory phase and fails to progress to the expected proliferative phase.[34] The role of low-grade, subclinical inflammation is being recognised in several disorders, such as irritable bowel syndrome and obesity, as well as in the general pathophysiology of gastrointestinal cancers.[35 36] The present work adds to this growing list, with the particularity that IL-17A/F mobilisation of chemokines-secreting neutrophils and monocytes was associated with poor anastomotic healing. Of note, excessive accumulation of neutrophils and monocytes has been shown to induce tissue damage and sustained inflammation, and to delay wound repair in several organs including the skin and the intestine.[37 38] Inflammation-induced damage in anastomotic wounds may be in part linked to a higher activation of collagenolytic enzymes. Accordingly, we found a higher expression of MMP-2 in poorly healing anastomotic wounds, which is known to be activated by TNF-α and IL-1β.[39 40] Other studies found an important role for MMP-9 in the healing of colonic anastomosis.[41 42] These studies and our findings further highlight the important role of heightened inflammation on the expression of matrix-degrading collagenases and AL.

Our approach led to the identification of several human-associated bacterial species that may modulate anastomotic healing. As a proof of principle, we show that strains of some bacterial species, namely *A. onderdonkii* and *P. goldsteinii*, which we found to adhere to the colonic mucosa, can directly affect the outcomes of colonic surgery in mice. More specifically, an increased abundance of *A. onderdonkii* is associated with impaired anastomotic healing and gut barrier. While no previous studies have confirmed a proinflammatory effect of this bacterium, one human study has shown that the abundance of the genus *Alistipes* is associated with the circulating levels of IL-17 in individuals at risk of metabolic syndrome.[43] Our findings suggest that not all members of *Alistipes* genus exhibit the same effects, since only *A. onderdonkii*, but not *A. indistinctus*, showed a proinflammatory activity. A strain of another bacterial species, *P. goldsteinii* kh35, had a beneficial effect on the recovery of gut injury by exerting the opposite effect, namely by inhibiting proinflammatory cytokines. Previous studies reported a beneficial effect of another *P. goldsteinii* strain that overlaps with our *P. goldsteinii* 1 ESV on metabolic health and obesity.[44] Overall, both *A. onderdonkii* and *P. goldsteinii* contain strains that can ultimately modulate the inflammatory response, suggesting that anastomotic healing might depend on an equilibrium between harmful and beneficial bacteria. While the identified bacteria constitute a proof-of-concept of the role of specific bacterial species in gut healing, other potential candidates require further investigation to add to the growing list of leak-associated[42] and healing-promoting bacteria (this study), the balance of which we show to be relevant to anastomotic healing.

Taken together, our findings open the possibility of identifying potential biological markers that could be measured in patients with CRC before their surgery to predict AL risk, since local gut inflammation has been shown to correlate with systemic low-grade inflammatory markers.[45] We show that blood cell counts and faecal lipocalin-2 could serve as valuable markers for the identification, before surgery, of patients at risk of developing AL. Faecal lipocalin-2 has been shown to be a sensitive marker able to detect very low-grade mucosal inflammation in patients with inflammatory bowel

disease and, as such, to be far more sensitive than the clinically used calprotectin.[46] Patients at risk of developing AL would be candidates for potential treatments before surgery targeting gut microbiota, such as prebiotics,[14 47] probiotics and postbiotics, to attenuate colonic inflammation, strengthen the gut barrier and improve anastomotic healing. Moreover, microbiota-based approaches could be relevant to other oncological and non-oncological gastrointestinal interventions, including small bowel resections, transanal tumour excision and gastroduodenal operations.

METHODS

Human studies

Patient recruitment and sample collection

Patients with CRC awaiting a colorectal surgical resection with anastomosis were recruited at the Digestive Surgery Service at the CHUM. Participants provided informed consent prior to samples and data acquisition. Prior to surgery, and before the administration of prophylactic antibiotics and mechanical bowel preparation, patients were requested to provide a fresh faecal sample following the standard operating procedures of the International Human Microbiome Standards project.[48] Samples were collected in hermetic containers with an anaerobic sachet (BBL GasPak anaerobic indicator, Becton, Dickinson and Company, Ontario, Canada) and stored at −80°C on arrival to the laboratory. During the operation, colonic mucosal samples (~ 1 cm^3) from the site adjacent to the anastomosis site were collected in a sterile manner, snap-frozen and stored at −80°C. At POD 3, rectal swabs were collected in PowerBead tubes (Qiagen, Toronto, Ontario, Canada) and stored at −80°C. Clinical data were collected from clinical charts. The diagnosis of AL after surgery was based on clinical or radiological evidence.

Animal experiments

Experiments were performed according to the guidelines of the Canadian Council of Animal Care and were approved by the Institutional Animal Care Committee of the Centre de recherche du Centre hospitalier de l'Université de Montréal (CRCHUM). Female mice were used in all experiments and were between 7 and 14 weeks at the time of surgery. C57BL/6 mice were bred at the CRCHUM animal facility in specific-pathogen-free (SPF) conditions. They were maintained under standard 12:12 light/dark conditions, housed at 3–5 mice per cage and were allowed ad libitum access to food and water. For knockout experiments, MyD88$^{-/-}$ (B6.129P2(SJL)-Myd88$^{tm1.1Defr}$/J), TNF-α$^{-/-}$ (B6.129S-Tnf^{tm1Gkl}/J) and wild-type control C57BL/6J mice were purchased from the Jackson Laboratory (Bar Harbor, Maine, USA) and maintained in the same conditions. Germ-free C57BL/6 female mice were purchased from the germ-free facility of the International Microbiome Centre at the University of Calgary, Alberta, Canada and housed at the gnotobiotic facility of the CRCHUM where the experiments were conducted. Mice with similar age and weight were randomly assigned to the study groups.

Faecal microbiota transplantation

Drinking water was supplemented with a mix of 3 antibiotics for 3 days before FMT. FMT was performed by administering 200 µL of faecal material suspended in sterile 0.9% saline (Baxter, Mississauga, Ontario, Canada) at 100 mg/mL by oral gavage and by applying 100 µL of the suspension on the animal's fur.[49] At day 14 after FMT, mice were sacrificed and gut parameters assessed, or were subjected to surgery by an operator blinded to the donor and intervention group.

Microbiome analysis

DNA extraction from faecal samples was performed using the Qiagen DNeasy PowerSoil kit according to the manufacturer's instructions. Primers for 16S rRNA gene amplification targeted the V5–V6 region: P609D (S-D-Bact-0785-a-S-18) 5'-GGMTTAGATACCCBDGTA-3'and P699R (S-*-Univ-1100-a-A-15) 5'-GGGTYKCGCTCGTTR-3'.[50] PCR amplification and sequencing were performed by Génome Québec, and the illumina MiSeq sequencing system platform was used for 2×250 bp paired-end sequencing of PCR products. Amplification was performed using the following conditions: initial denaturation at 94°C for 2 min, denaturation at 94°C for 30 s, annealing at 58°C for 30 s, extension at 72°C for 30 s, final extension at 72°C for 7 min, 4°C hold, over 35 cycles. Reagent controls were below the detection limit used by Génome Québec for quality assurance. The Anchor pipeline[51] was used to process amplicon sequences. Briefly, Mothur[52] was used to align and dereplicate sequences before selection of ESVs using a count threshold of 100 across all samples. Annotation queried two sequence repositories with strict BLASTn criteria (>99% identity and coverage): National Center for Biotechnology Information (NCBI) curated bacterial and Archaea RefSeq, and NCBI nt. Database versions were from January 2021; all annotation is considered putative and subject to improvement as database errors are resolved and new species are characterised. Raw sequence data have been deposited at the NCBI accession: Sequence Read Archive Project ID (PRJNA848219).

Statistical analysis

Statistical analysis was performed using Prism 9V.9.3.0 (GraphPad Software, San Diego, California, USA) and R (V.4.1.0). Logarithmic transformation was performed when normality or equality of variances could not be assumed. Intergroup comparisons were performed using two-tailed Student's t-test or Mann-Whitney U test. For multiple groups analysis, one-way analysis of variance was performed with post hoc Tukey's test or Kruskal-Wallis test with Dunn's post hoc test. In experiments with FMT, to prevent overestimation of the association due to pseudoreplication, the biological unit consisted of the donor (N=1 donor) and mice colonised from one donor were considered replicates.[53] Therefore, to account for correlation between measurements from mice recolonised by FMT from the same donor, generalised estimating equations were applied using the geeglm function from the geepack R package[54] (V.1.3–2) with the family parameter set to 'binomial' or 'gaussian' and the potential correlation structure among donor-matching mice samples was specified as 'independent'. Significance between parameters between groups was assessed with a Wald test.

Data and materials availability

NCBI accession: Sequence Read Archive Project ID (PRJNA848219).

Author affiliations
[1]Nutrition and Microbiome Laboratory, Centre de recherche du Centre hospitalier de l'Université de Montréal (CRCHUM), Montréal, Québec, Canada
[2]Digestive Surgery Service, Centre hospitalier de l'Université de Montréal (CHUM), Montréal, Québec, Canada

[3]Department of Surgery, Université de Montréal, Montréal, Québec, Canada
[4]Institut du cancer de Montréal, Montréal, Québec, Canada
[5]Canadian Centre for Computational Genomics, McGill Genome Centre, Department of Human Genetics, McGill University, Montréal, Québec, Canada
[6]Gerald Bronfman Department of Oncology, McGill University, Montréal, Québec, Canada
[7]Molecular Oncology Laboratory, Department of Chemistry, Université du Québec à Montréal (UQAM), Montréal, Québec, Canada
[8]Axe Cancer, Centre de recherche du Centre hospitalier de l'Université de Montréal (CRCHUM), Montréal, Québec, Canada
[9]Laboratory of Immunotherapy and Oncomicrobiome, Centre de recherche du Centre hospitalier de l'Université de Montréal (CRCHUM), Montréal, Québec, Canada
[10](Current address: Department of General Surgery, King Fahd Hospital of the University, College of Medicine, Imam Abdulrahman Bin Faisal University, Dammam, Saudi Arabia). Digestive Surgery Service, Centre hospitalier de l'Université de Montréal (CHUM), Montréal, Québec, Canada
[11]Division of General Surgery, Université de Montréal, Montréal, Québec, Canada
[12]Department of Medicine, Faculty of Medicine, Université de Montréal, Montréal, Québec, Canada
[13]Renal Division, Department of Medicine, Centre hospitalier de l'Université de Montréal (CHUM), Montréal, Québec, Canada
[14]Hemato-oncology Division, Centre Hospitalier de l'Université de Montréal (CHUM), Montréal, Québec, Canada
[15]School of Biology and Environmental Science, University College Dublin, Dublin, Ireland
[16]Institut de Recherche en Biologie Végétale, Université de Montréal, Montréal, Québec, Canada

Twitter Roy Hajjar @Roy__Hajjar, Emmanuel Gonzalez @GonzalezEmBio, Nicholas J B Brereton @NJBBrereton and Manuela M Santos @Nut_Microb_Lab

Acknowledgements We thank the Génome Québec sequencing platform, Hélène Héon, Maryse Boulay, Stefanie Beaulieu, Avila Croisetière, Marie-Claude Therrien, Geneviève Lauzon and Christian Demers from the CRCHUM animal and gnotobiotic facility, Julien Lamontagne and Alexia Grangeon from the CRCHUM metabolomics platform, Feryel Azzi, Liliane Meunier, and Véronique Barrès from the Molecular Pathology core facility of the CRCHUM, Josée Tessier from the Surgical Training Unit at the Hôpital Maisonneuve-Rosemont, Sabrina Lavoie from the CRCHUM and Jacqueline Chung for editing the manuscript. Banking was done in collaboration with the Réseau de recherche sur le cancer (Fonds de la Recherche du Québec - Santé) that is affiliated with the Canadian Tumor Repository Network (CTRNet).

Contributors Conceptualisation: RH, CR, MMS. Methodology: RH, EG, MO, AAA, GF, AC, HVR, SD, TC, PL, CG, ASA, KD, NT, ST, FS, HA, FD, RL, HS, FS, RW, RR, ED, BR, J-FC, BA, NJBB, CR, MMS. Visualisation: RH, EG, TC, MMS. Supervision: CR, MMS. Original draft: RH, MMS. Review and editing: RH, EG, MO, AAA, GF, AC, HVR, SD, TC, PL, CG, ASA, KD, NT, ST, FS, HA, FD, RL, HS, FS, RW, RR, ED, BR, J-FC, BA, NJBB, CR, MMS. Overall supervisor and guarantor: MMS.

Funding Canadian Institutes of Health Research grants FRN-159775 and PJT-175181 (MMS). Natural Sciences and Engineering Research Council of Canada grants RGPIN-2018-06442 (MMS). New Frontiers in Research Fund – Exploration grant NFRFE-2020-00991 (MMS, CR). Canadian Society of Colon and Rectal Surgeons operating grant 2019 (CR, RH). Fonds de recherche du Québec – Santé (FRQ-S) and Ministère de la Santé et des Services sociaux Resident Physician Health Research Career Training Program (RH). Canadian Institutes of Health Research Graduate Scholarships program (RH). Institut du cancer de Montréal (Canderel scholarship) (MO, TC, CG, ASA). Fonds de recherche du Québec – Santé (FRQ-S) (Postdoctoral Fellowship) (KD). BA holds a Chair in Cancer Prevention and Treatment at UQAM

Competing interests None declared.

Patient and public involvement Patients and/or the public were involved in the design, or conduct, or reporting, or dissemination plans of this research. Refer to the Methods section for further details.

Patient consent for publication Not applicable.

Ethics approval This study involves human participants and was approved by Research Ethics Board of the Centre hospitalier de l'Université de Montréal (CHUM) (numbers: 19.021, 21.359, 21,153 and 21.368). Participants gave informed consent to participate in the study before taking part.

Provenance and peer review Not commissioned; externally peer reviewed.

Data availability statement All data relevant to the study are included in the article or uploaded as online supplemental information.

ORCID iDs
Roy Hajjar http://orcid.org/0000-0002-3768-3402
Nicholas J B Brereton http://orcid.org/0000-0002-2434-3249
Manuela M Santos http://orcid.org/0000-0003-3497-0585

REFERENCES

1 Siegel RL, Miller KD, Fuchs HE, *et al*. Cancer statistics, 2022. *CA Cancer J Clin* 2022;72:7–33.
2 Zhao S, Zhang L, Gao F, *et al*. Transanal drainage tube use for preventing anastomotic leakage after laparoscopic low anterior resection in patients with rectal cancer: a randomized clinical trial. *JAMA Surg* 2021;156:1151–8.
3 Mirnezami A, Mirnezami R, Chandrakumaran K, *et al*. Increased local recurrence and reduced survival from colorectal cancer following anastomotic leak: systematic review and meta-analysis. *Ann Surg* 2011;253:890–9.
4 Krarup P-M, Nordholm-Carstensen A, Jorgensen LN, *et al*. Anastomotic leak increases distant recurrence and long-term mortality after curative resection for colonic cancer: a nationwide cohort study. *Ann Surg* 2014;259:930–8.
5 van der Stok EP, Spaander MCW, Grünhagen DJ, *et al*. Surveillance after curative treatment for colorectal cancer. *Nat Rev Clin Oncol* 2017;14:297–315.
6 Salvans S, Mayol X, Alonso S, *et al*. Postoperative peritoneal infection enhances migration and invasion capacities of tumor cells in vitro: an insight into the association between anastomotic leak and recurrence after surgery for colorectal cancer. *Ann Surg* 2014;260:939–43.
7 Bachmann R, Leonard D, Delzenne N, *et al*. Novel insight into the role of microbiota in colorectal surgery. *Gut* 2017;66:738–49.
8 Hooper LV, Wong MH, Thelin A, *et al*. Molecular analysis of commensal host-microbial relationships in the intestine. *Science* 2001;291:881–4.
9 Bäckhed F, Ley RE, Sonnenburg JL, *et al*. Host-Bacterial mutualism in the human intestine. *Science* 2005;307:1915–20.
10 Guyton K, Alverdy JC. The gut microbiota and gastrointestinal surgery. *Nat Rev Gastroenterol Hepatol* 2017;14:43–54.
11 Guarner F, Malagelada J-R. Gut flora in health and disease. *The Lancet* 2003;361:512–9.
12 Meneghin A, Hogaboam CM, disease I. The innate immune response, and fibrosis. *J Clin Invest*
13 Souza DG, Vieira AT, Soares AC, *et al*. The essential role of the intestinal microbiota in facilitating acute inflammatory responses. *J Immunol* 2004;173:4137–46.
14 Hajjar R, Oliero M, Cuisiniere T, *et al*. Improvement of colonic healing and surgical recovery with perioperative supplementation of inulin and galacto-oligosaccharides. *Clin Nutr* 2021;40:3842–51.
15 Karmarkar D, Rock KL. Microbiota signalling through MyD88 is necessary for a systemic neutrophilic inflammatory response. *Immunology* 2013;140:483–92.
16 Hunter MV, Lee DM, Harris TJC, *et al*. Polarized E-cadherin endocytosis directs actomyosin remodeling during embryonic wound repair. *J Cell Biol* 2015;210:801–16.
17 Minerbi A, Gonzalez E, Brereton NJB, *et al*. Altered microbiome composition in individuals with fibromyalgia. *Pain* 2019;160:2589–602.
18 Parker BJ, Wearsch PA, Veloo ACM, *et al*. The Genus *Alistipes*: Gut Bacteria With Emerging Implications to Inflammation, Cancer, and Mental Health. *Front Immunol* 2020;11:906.
19 Hernández-Chirlaque C, Aranda CJ, Ocón B, *et al*. Germ-Free and antibiotic-treated mice are highly susceptible to epithelial injury in DSS colitis. *J Crohns Colitis* 2016;10:1324–35.
20 Grover M, Kashyap PC. Germ-Free mice as a model to study effect of gut microbiota on host physiology. *Neurogastroenterol Motil* 2014;26:745–8.
21 Lai H-C, Lin T-L, Chen T-W, *et al*. Gut microbiota modulates COPD pathogenesis: role of anti-inflammatory *Parabacteroides goldsteinii* lipopolysaccharide. *Gut* 2022;71:309–21.
22 Liu T, Zhang L, Joo D, *et al*. NF-κB signaling in inflammation. *Sig Transduct Target Ther*
23 Telem DA, Chin EH, Nguyen SQ, *et al*. Risk factors for anastomotic leak following colorectal surgery: a case-control study. *Arch Surg* 2010;145:371–6.
24 McGinley AM, Sutton CE, Edwards SC, *et al*. Interleukin-17A serves a priming role in autoimmunity by recruiting IL-1β-Producing myeloid cells that promote pathogenic T cells. *Immunity* 2020;52:342–56.
25 Neurath MF. New targets for mucosal healing and therapy in inflammatory bowel diseases. *Mucosal Immunol* 2014;7:6–19.
26 Coccia M, Harrison OJ, Schiering C, *et al*. IL-1β mediates chronic intestinal inflammation by promoting the accumulation of IL-17A secreting innate lymphoid cells and CD4(+) Th17 cells. *J Exp Med* 2012;209:1595–609.
27 Koelink PJ, Overbeek SA, Braber S, *et al*. Collagen degradation and neutrophilic infiltration: a vicious circle in inflammatory bowel disease. *Gut* 2014;63:578–87.

28 Landén NX, Li D, Ståhle M. Transition from inflammation to proliferation: a critical step during wound healing. *Cell Mol Life Sci* 2016;73:3861–85.
29 Palmisano S, Campisciano G, Iacuzzo C, *et al*. Role of preoperative gut microbiota on colorectal anastomotic leakage: preliminary results. *Updates Surg* 2020;72:1013–22.
30 van Praagh JB, de Goffau MC, Bakker IS, *et al*. Mucus microbiome of anastomotic tissue during surgery has predictive value for colorectal anastomotic leakage. *Ann Surg* 2019;269:911–6.
31 Sparreboom CL, Wu Z-Q, Ji J-F, *et al*. Integrated approach to colorectal anastomotic leakage: communication, infection and healing disturbances. *World J Gastroenterol* 2016;22:7226–35.
32 Jin X, Liu Y, Yan W, *et al*. Gut microbiota from nCAL patients promotes colon anastomotic healing by inducing collagen synthesis in epithelial cells. *J Gastroenterol Hepatol* 2022;37:1756–67.
33 Zhang M, Sun K, Wu Y, *et al*. Interactions between intestinal microbiota and host immune response in inflammatory bowel disease. *Front Immunol* 2017;8:942. doi:10.3389/fimmu.2017.00942
34 Morgan RB, Shogan BD. The science of anastomotic healing. *Semin Colon Rectal Surg* 2022;33. doi:10.1016/j.scrs.2022.100879. [Epub ahead of print: 08 03 2022].
35 Guinane CM, Cotter PD. Role of the gut microbiota in health and chronic gastrointestinal disease: understanding a hidden metabolic organ. *Therap Adv Gastroenterol* 2013;6:295–308.
36 Wu H, Ballantyne CM. Metabolic inflammation and insulin resistance in obesity. *Circ Res* 2020;126:1549–64.
37 Takagi N, Kawakami K, Kanno E, *et al*. Il-17A promotes neutrophilic inflammation and disturbs acute wound healing in skin. *Exp Dermatol* 2017;26:137–44.
38 Jones G-R, Bain CC, Fenton TM, *et al*. Dynamics of colon monocyte and macrophage activation during colitis. *Front Immunol* 2018;9:2764.
39 Yang Y-N, Wang F, Zhou W, *et al*. TNF-α stimulates MMP-2 and MMP-9 activities in human corneal epithelial cells via the activation of FAK/ERK signaling. *Ophthalmic Res* 2012;48:165–70.
40 Mountain DJH, Singh M, Menon B, *et al*. Interleukin-1Beta increases expression and activity of matrix metalloproteinase-2 in cardiac microvascular endothelial cells: role of PKCalpha/beta1 and MAPKs. *Am J Physiol Cell Physiol* 2007;292:C867–75.
41 van Praagh JB, Luo JN, Zaborina O, *et al*. Involvement of the Commensal Organism *Bacillus subtilis* in the Pathogenesis of Anastomotic Leak. *Surg Infect* 2020;21:865–70.
42 Shogan BD, Belogortseva N, Luong PM, *et al*. Collagen degradation and MMP9 activation by *Enterococcus faecalis* contribute to intestinal anastomotic leak. *Sci Transl Med* 2015;7:ra68.
43 Zhou X, Johnson JS, Spakowicz D, *et al*. Longitudinal Analysis of Serum Cytokine Levels and Gut Microbial Abundance Links IL-17/IL-22 With *Clostridia* and Insulin Sensitivity in Humans. *Diabetes* 2020;69:1833–42.
44 Wu T-R, Lin C-S, Chang C-J, *et al*. Gut commensal *Parabacteroides goldsteinii* plays a predominant role in the anti-obesity effects of polysaccharides isolated from *Hirsutella sinensis*. *Gut* 2019;68:248-–62.
45 Køstner AH, Nielsen PS, Georgsen JB, *et al*. Systemic inflammation associates with a myeloid inflamed tumor microenvironment in primary resected colon Cancer-May cold tumors simply be too hot? *Front Immunol* 2021;12:716342.
46 Zollner A, Schmiderer A, Reider SJ, *et al*. Faecal biomarkers in inflammatory bowel diseases: calprotectin versus Lipocalin-2-a comparative study. *J Crohns Colitis* 2021;15:43–54.
47 Hajjar R, Richard CS, Santos MM. The role of butyrate in surgical and oncological outcomes in colorectal cancer. *Am J Physiol Gastrointest Liver Physiol* 2021;320:G601–8.
48 Dore J, Ehrlich SD, Levenez F, *et al*. IHMS Consortium (2015), IHMS_SOP 03 V1: standard operating procedure for fecal samples self-collection, laboratory analysis handled within 4 to 24 hours (4 hours <x ≤ 24 hours). International human microbiome standards. Available: http://www.microbiome-standards.org
49 Routy B, Le Chatelier E, Derosa L, *et al*. Gut microbiome influences efficacy of PD-1-based immunotherapy against epithelial tumors. *Science* 2018;359:91–7.
50 Klindworth A, Pruesse E, Schweer T, *et al*. Evaluation of general 16S ribosomal RNA gene PCR primers for classical and next-generation sequencing-based diversity studies. *Nucleic Acids Res* 2013;41::e1.
51 Gonzalez E, Pitre FE, Brereton NJB. Anchor: a 16S rRNA gene amplicon pipeline for microbial analysis of multiple environmental samples. *Environ Microbiol* 2019;21:2440–68.
52 Schloss PD, Westcott SL, Ryabin T, *et al*. Introducing mothur: open-source, platform-independent, community-supported software for describing and comparing microbial communities. *Appl Environ Microbiol* 2009;75:7537–41.
53 Walter J, Armet AM, Finlay BB, *et al*. Establishing or Exaggerating causality for the gut microbiome: lessons from human Microbiota-Associated rodents. *Cell* 2020;180:221–32.
54 Højsgaard S, Halekoh U, Yan J. The R package geepack for generalized estimating equations. *Journal of Statistical Software* 2005;15:1–11.

Supplementary materials

Supplementary methods

Retrospective review

The charts of patients with confirmed AL after a colorectal resection for CRC at the CHUM between 2011 and 2021 were identified and reviewed. Charts of patients undergoing resection for CRC during the same period, and who did not develop AL, were randomly selected and reviewed. The following cases were excluded: no anastomosis, perforated tumor or intestinal perforation before surgery, emergency surgery for bowel obstruction, active confirmed infection, hematological malignancy, hyperthermic intraperitoneal chemotherapy, palliative surgery, and no available preoperative complete blood count within 3 months before surgery. To prevent misclassification, charts were screened, and data was collected and validated by two independent individuals, and random data verification was further performed.

Surgical intervention

At day 4 after FMT, mice were subjected to surgery as previously described (1). They were followed postoperatively and sacrificed on postoperative day (POD) 6. On the day of surgery, mice received a subcutaneous injection of the analgesic buprenorphine-sustained-release (1 mg/Kg, Chiron Compounding Pharmacy Inc, Guelph, ON, Canada), then underwent general anesthesia with isoflurane (2-3%). The abdomen was shaved, and the skin was disinfected with 3 passages of 10% povidone-iodine and 70% ethanol solutions. An abdominal subcutaneous injection of the local anesthetic bupivacaine 0.25% (2 mg/Kg, Aspen Pharmacare Canada Inc, Oakville, ON, Canada) was performed at the incision site. A midline abdominal 2 cm laparotomy incision was performed. The cecum was localized and exteriorized, and a colotomy was performed by

Hajjar R, *et al. Gut* 2022;0:1–12. doi: 10.1136/gutjnl-2022-328389

transecting 80% of the circumference of the proximal colon, distal to the cecum. The colotomy was then closed with 6 interrupted sutures of polypropylene 8-0. Under direct vision, the integrity of the repair was tested with rectal administration of warm sterile saline via a 22G plastic cannula. The abdomen was closed in 2 layers, with one running suture at the muscle level, and one subcuticular running suture at the skin level. Intraoperatively, the respiratory rate was continuously monitored, and mice were maintained on oxygen (0.5 L/min) and on a heating pad. They were resuscitated with subcutaneous warm 0.9% NaCl/5% Dextrose (40 mL/Kg, Baxter). After surgery, mice were housed in cages with soft bedding material. Drinking water was supplemented with acetaminophen 32 mg/mL (Tempra, Paladin Labs Inc., St-Laurent, QC, Canada) to optimize analgesia, and mice were assessed daily until sacrifice. Signs of sepsis or other surgical complications, including difficulty breathing, failure to move when touched, weight loss greater than 20% or wound dehiscence, were set as intervention points to proceed with urgent euthanasia.

Antibiotic treatment

Drinking water was supplemented during all the experimental period with a mix of 3 antibiotics: ampicillin (1 mg/ml, WISENT Inc., QC, Canada), streptomycin (5 mg/ml, Sigma-Aldrich/MilliporeSigma Canada Co, ON, Canada) and colistin (1 mg/ml, SteriMax Inc., ON, Canada) (2). The control group received sterile drinking water.

Macroscopic anastomotic healing

Macroscopic healing of the anastomosis was performed using the anastomotic leak (AL) score as follows: 0, normal healing; 1, flimsy adhesion; 2, dense adhesion; 3, phlegmon/abscess; 4, overt

Hajjar R, *et al. Gut* 2022;0:1–12. doi: 10.1136/gutjnl-2022-328389

leak with peritonitis (1,3-5). Grading was performed by 3 independent evaluators blinded to the intervention group.

Bacterial supplementation

Alistipes onderdonkii kh33*, Alistipes indistinctus* kh34 *and Parabacteroides goldsteinii* kh35 (CHUM Research Center collection numbers 417, 416 and 418) were grown on tryptone soy agar plates with 5% sheep blood (Oxoid, Thermo Fischer Scientific inc., ON, Canada) at 37°C in anaerobic conditions for 48 hours. On the day of gavage, bacterial colonies were scraped and suspended in 0.9% saline (Baxter) at an optical density at 600 nm of 1.0. Bacterial supplementation was performed by administering a daily oral gavage of 200 µL of the fresh suspension for 2 days before surgery. Control mice received saline. Bacterial identity of the culture was routinely monitored by real-time quantitative polymerase chain reaction (qPCR) using primers listed in **Table S2**, and by matrix-assisted laser desorption ionization time-of-flight (MALDI-TOF) mass spectrometry. Confirmation of bacterial colonization was performed on fecal samples by qPCR.

Cytokines treatment

Before surgery, mice received an intraperitoneal (i.p.) injection of the recombinant mouse tumor necrosis factor alpha (TNF-α) protein (500 ng in 200 µL of PBS, R&D Systems Inc., Toronto, ON, Canada) or of a mix of the recombinant mouse macrophage inflammatory protein 1 alpha (MIP-1α), monocyte chemoattractant protein 1 (MCP-1) and macrophage inflammatory protein 2 (MIP-2) (500 ng of each in a total volume of 200 µL of PBS, R&D Systems Inc.). For TNF-α depletion, mice received an i.p. injection of the mouse anti-TNF-α monoclonal antibody (0.5 mg,

clone XT3.11, BioXCell, NH, USA), or of a control isotype (0.5 mg, rat IgG1 isotype control, anti-horseradish peroxidase, BioXCell), the day before the operation.

Tissue and feces homogenization

Anastomotic tissue was homogenized in distilled water for hydroxyproline quantification. For the other measurements, anastomotic tissue and feces were homogenized on ice in lysis buffer (Tris-HCl pH 7.5, NaCl, Nonidet P-40, H_2O, and protease inhibitor). Protein concentration was quantified using the Pierce™ BCA Protein Assay Kit (Thermo Fischer Scientific, MA, USA).

Gelatin zymography

Gelatin zymography was used to assess the hydrolytic activities of colonic collagenases at the wound site. Briefly, homogenates of anastomotic tissue (10 μg of proteins) were subjected to SDS-PAGE in a gel containing 0.1 mg/ml gelatin (G2625, Sigma-Aldrich/MilliporeSigma Canada Co). The gels were then incubated in 2.5% Triton X-100 (BioShop Canada Inc., TRX506.500, ON, Canada) and rinsed in nanopure distilled water. Gels were further incubated at 37°C for 20 h in 20 mM NaCl, 5 mM $CaCl_2$, 0.02% Brij-35, 50 mM Tris–HCl buffer, pH 7.6 and then stained with 0.1% Coomassie Brilliant blue R-250 (CBB250, BioShop Canada Inc., ON, Canada) and destained in 10% acetic acid, 30% methanol in water. Gelatinolytic activity was detected as unstained bands on a blue background using ImageJ (6).

Depletion of neutrophiles and monocytes

Mice underwent FMT as previously described with a pooled fecal sample (100 mg/mL) from 4 donors with AL (Table S1, donors 11, 13, 17 and 18). To deplete neutrophiles, mice received an

intraperitoneal injection of the mouse anti-Ly6G monoclonal antibody (clone 1A8, 200 µg, BioXCell) or of the rat IgG2a isotype control (clone 2A3, 200 µg, BioXCell) at day 13 after FMT. To deplete monocytes, mice received an intravenous injection of clodronate liposomes (1 mg in 200 µL, Liposoma BV, Amsterdam, The Netherlands) or control liposomes containing PBS (200 µL, Liposoma BV) at day 12 after FMT.

Quantification of hydroxyproline

The concentration of hydroxyproline was quantified in anastomotic colonic tissue using a colorimetric hydroxyproline assay kit (ab222941, Abcam Inc., Toronto, ON, Canada) following the manufacturer's recommendations. The concentration of hydroxyproline was adjusted to the weight of homogenized tissue.

Quantification of fibronectin and E-cadherin

Fibronectin and E-cadherin were quantified by an enzyme-linked immunosorbent assay (ELISA) at the anastomosis site (ab108849, ab197751, Abcam Inc.) and was adjusted to the total protein concentration.

Splenic bacterial load assessment

The spleen was collected in a sterile fashion. Bacterial load was estimated in splenic tissue by culturing and counting colony forming units (CFUs). Total sterile splenic tissue was homogenized in 200 µL of sterile 0.9% saline (Baxter), diluted 10-fold, and 200 µL of the homogenate plated on tryptone soy agar plates with 5% sheep blood (Oxoid, Thermo Fischer Scientific inc.) at 37°C in aerobic condition. CFUs were quantified at 72 hours.

Cytokine quantification

Inflammatory cytokines were quantified in colonic homogenates using a multiplex assay (Meso Scale Diagnostics, Rockville, MD, USA), or enzyme-linked immunosorbent assay (ELISA) for MIP-2, lipocalin-2, and calprotectin (DY452, DY1757 and DS8900, R&D Systems, Inc.) and were corrected for protein concentration.

16S rRNA gene sequencing

Sanger sequencing of the 16S rRNA gene of *P. goldsteinii* kh35 was performed at the Centre d'expertise et de services Génome Québec using the primers 27F (AGAGTTTGATCMTGGCTCAG) and 1492R (TACGGYTACCTTGTTACGACTT), and alignment of the variable V5-V6 region was performed using NCBI BLASTn (7).

Complete blood count

Blood samples were retrieved by terminal retro-orbital puncture in tubes with EDTA (BD Microtainer blood collection tubes, Becton, Dickinson and Company). Complete blood counts (CBC) were measured using an automated cell counter calibrated for murine samples (ABC vet counter, ABX Hématologie, Montpellier, France).

Flow cytometry

Blood was collected in lithium heparin tubes (BD Microtainer blood collection tubes, Becton, Dickinson and Company) as previously described (8). After red blood cell lysis using ACK buffer, leukocytes were blocked with anti CD16/CD32 antibodies (Fc block, Becton, Dickinson and Company) for 15 minutes, washed and then stained for 30 minutes with the following fluorescent

Hajjar R, *et al. Gut* 2022;0:1–12. doi: 10.1136/gutjnl-2022-328389

antibodies: F4/80-PE from (Miltenyi Biotech Inc., Auburn, CA, USA) and CD11b-AF700, Ly6C-FITC and Ly6G-APC-H7 (Becton, Dickinson and Company). Live cells were isolated using the LIVE/DEAD™ Fixable Aqua Dead Cell Stain Kit (Invitrogen, Thermo Fischer Scientific inc.). Cells were immediately passed through a flow cytometer (BD LSRFortessa™ Cell Analyzer, Becton, Dickinson and Company) and then analyzed using FlowJo v10.3 (FlowJo, LLC, Becton, Dickinson and Company).

Diversity and differential abundance analysis

Alpha diversity was measured using Shannon diversity indices with the Phyloseq package and was compared between groups with *t*-tests. Unconstrained Principal component analysis (PCA) ordination and constrained Redundancy analysis (RDA) was performed on rlog-transformed exact sequence variant (ESV) abundance using the Phyloseq package and dispersion ellipses were drawn using the veganCovEllispse function from the Vegan package in R (9,10). Significance of the different constraints in the RDA analysis was evaluated using ANOVA-like permutation test (vegan package). Differential abundance analysis on 16S rRNA gene amplicons was performed using DESeq2 (11), which can perform well with uneven library sizes and sparsity common to 16S rRNA gene data. Sparsity and low-count cut-offs were applied whereby an ESV count in a single sample is < 90% of the count in all samples, and ESV counts must be > 2 in 40% of the samples. For significance, a false discovery rate (Benjamini-Hochberg procedure) < 0.05 was applied.

Statistical learning

Logistic regression for the classification of non-AL controls and AL patients using ESV abundance was based on a statistical learning algorithm using a Train-Valid-Test data split involving two

Hajjar R, *et al. Gut* 2022;0:1–12. doi: 10.1136/gutjnl-2022-328389

steps. Box-Cox transformation of the ESV counts was estimated prior to training using caret R library (Max Kuhn (2021). caret: Classification and Regression Training. R package version 6.0-88). In the first step, explanatory variables (ESVs) were selected by estimating the predictive power of different subsets of differentially abundant ESVs. To control for model overfitting, a 10-fold cross validation procedure was carried out using different sets of samples for training and validation, picked randomly a thousand times. The best predictive explanatory variables were selected for the second step. Explanatory performance of the best predictor sets was assessed using the mice ESV counts as training set and human donors ESV counts as test set. Prediction of AL/No-AL outcome on the full donor dataset was estimated, and accuracy, sensitivity, and specificity were calculated from a confusion table.

Cell experiments

The human monocyte cell line THP-1 (ATCC© TIB-202™) was grown at 37°C in 5% CO_2 atmosphere in Roswell Park Memorial Institute (RPMI) medium supplemented with 10% heat inactivated fetal bovine serum (FBS) (WISENT Inc., QC, Canada). *P. goldsteinii* kh35 and *A. onderdonkii* kh33 were grown in RPMI with 10% heat inactivated FBS for 48 hours in anaerobic conditions. The bacterial suspension was then centrifuged, and the supernatant filtered using a 0.2 μm filter. THP-1 cells were pretreated for 2 hours with 100% *P. goldsteinii* kh35 or *A. onderdonkii* kh33 supernatant or with filtered medium as control. Cells incubated with *P. goldsteinii* kh35 supernatant were additionally exposed for 1 hour to lipopolysaccharide (LPS) from *Escherichia coli* O55:B5 (1 μg/ml, Sigma-Aldrich/MilliporeSigma Canada Co).

DNA and RNA extraction

Fecal, mucosal and splenic DNA was extracted using the Qiagen DNeasy PowerSoil® kit (Qiagen, Toronto, ON) and quantified using a spectrophotometer (DeNovix DS-11 FX, Wilmington, DE). Total RNA from THP-1 cells was extracted using TRIzol reagent (Invitrogen, Thermo Fischer Scientific inc.). Reverse transcription was performed using the high-capacity cDNA Reverse Transcription Kit (Thermo Fischer Scientific inc.).

Quantitative PCR

qPCR was performed using the PowerUp™ SYBR™ Green Master Mix (Applied Biosystems™, Thermo Fisher Scientific inc.) in a Rotor Gene 3000A (Corbett Research, Australia) as previously reported (12). The primers are listed in **Table S2**. mRNA expression was normalized to β-actin.

Nuclear factor kappa B (NF-κB) activity

THP1-Lucia™ NF-κB Cells (InvivoGen, San Diego, CA, USA) were grown in RPMI with 10% heat inactivated FBS, 100 µg/ml Normocin™ (InvivoGen), Pen-Strep (100 U/mL-100 µg/mL, WISENT Inc., QC, Canada) with Zeocin® (100 µg/ml, InvivoGen) every 2 passages. For the assay, cells were seeded at $4x10^5$ cells/mL of medium in a 24-well plate. They were pre-treated with *P. goldsteinii* kh35 supernatant or control medium for 2 hours, then treated with 1 µg/ml of *E. coli* LPS O55:B5 for 24 hours. 50 µL of the medium was collected and luciferase expression was measured by adding 50 µl of QUANTI-Luc reagent (InvivoGen) in a white 96-well plate. Readings are performed using the Spark® multimode microplate reader (Tecan Group Ltd., Switzerland).

Hajjar R, *et al. Gut* 2022;0:1–12. doi: 10.1136/gutjnl-2022-328389

Western blot

THP-1 cells were centrifuged at 800 g for 5 minutes and resuspended in 100 µl of 1x western blot loading buffer, heated at 95°C for 5 minutes, and loaded on a 10% SDS-PAGE gel. After migration, proteins are transferred on a Nitrocellulose Membrane 0.45 µM (Bio-Rad Laboratories (Canada) Ltd., Mississauga, ON, Canada), blocked using 5% skim milk (BioShop Canada Inc., Burlington, ON, Canada) in TBS-T (Tris buffered saline-0.05%/Tween-20) for 1 hour at room temperature. The membrane was then incubated with MyD88 rabbit mAb (#4283, Cell Signaling, New England Biolabs, Ltd., Whitby, ON, Canada) in 5% bovine serum albumin (BSA) in TBS-T overnight at 4°C. The membrane was washed for 5 minutes in TBS-T with agitation at room temperature and incubated with goat anti-rabbit IgG (H+L) secondary antibody (Invitrogen, Thermo Fischer Scientific inc.) for 1 hour at room temperature. The membrane was then washed for 5 minutes in TBS-T at room temperature, developed with SuperSignal™ West Pico PLUS Chemiluminescent Substrate (Thermo Fischer Scientific inc.), and exposed using a ChemiDoc System (Bio-Rad Laboratories (Canada) Ltd., Mississauga, ON, Canada). Bands were quantified using Image Lab (version 6.0.1, Bio-Rad Laboratories (Canada) Ltd.).

Hajjar R, *et al. Gut* 2022;0:1–12. doi: 10.1136/gutjnl-2022-328389

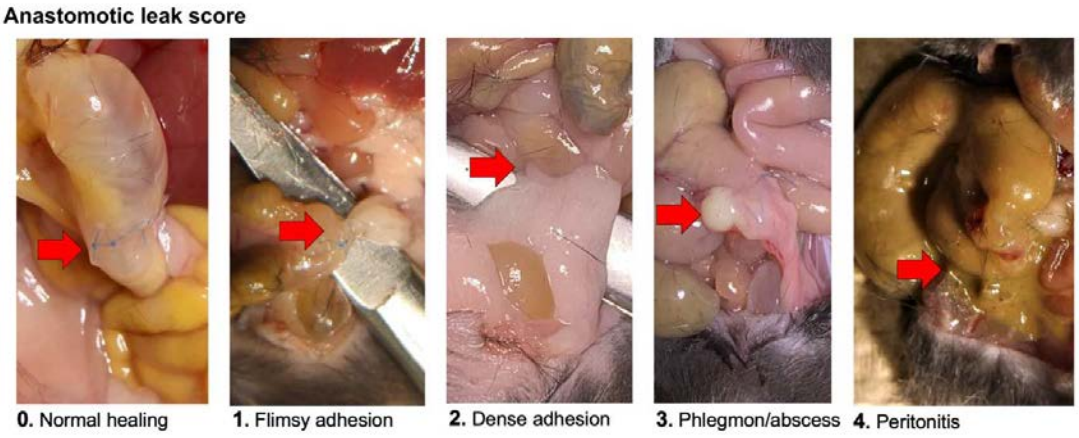

Supplementary figure 1. Anastomotic leak (AL) score used to assess anastomotic healing. Level 0 indicates optimal healing without anastomotic adhesions. Level 1 indicates light adhesions of abdominal fatty tissue with the anastomotic wound. Level 2 depicts dense adhesions of abdominal fatty tissue or organs with the anastomosis. Level 3 implies the presence of a local infectious process involving a phlegmon or abscess. Level 4 indicates an overt anastomotic leak of intestinal content with fecal peritonitis. Red arrows indicate the site of the anastomosis.

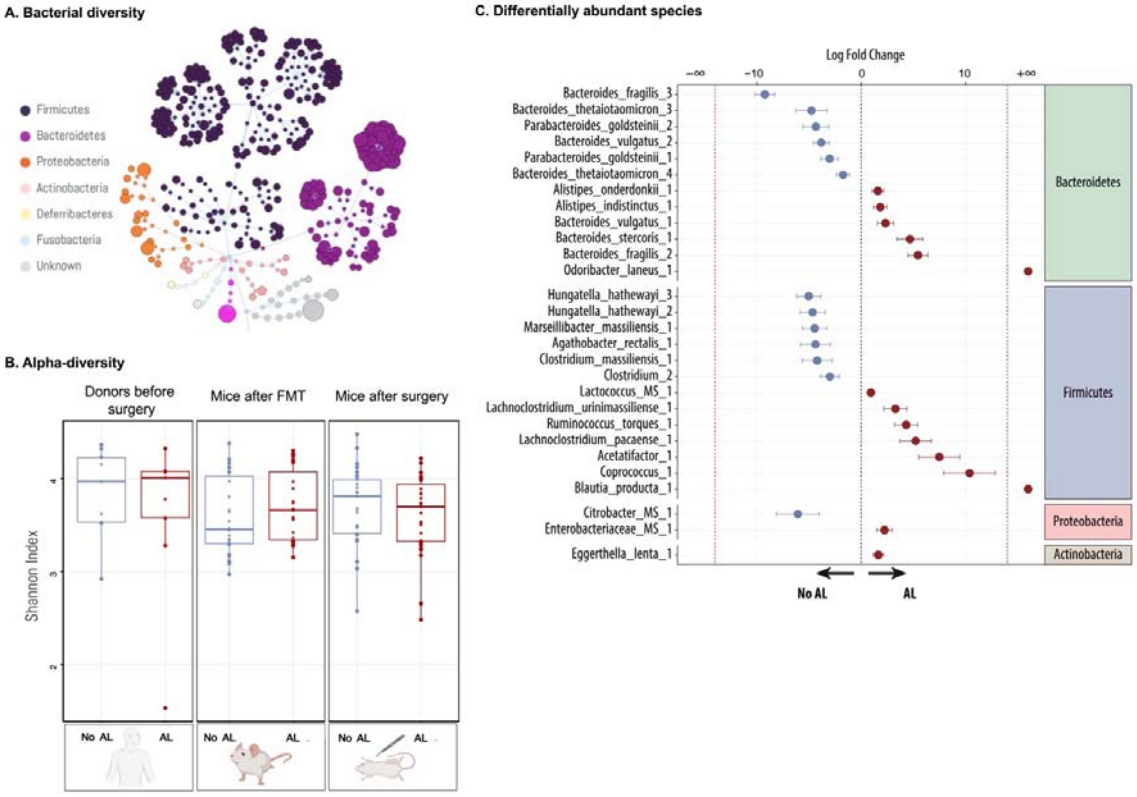

Supplementary figure 2. Gut microbiota of donors and FMT mice. (**A**) Bacterial diversity diagram representing the full set of ESVs organized in a hierarchical data structure based on their taxonomy as determined by 16S ribosomal RNA gene sequencing and the ANCHOR pipeline. (**B**) Shannon index. (**C**) Differential abundance (DESeq2 *p*-adj < 0.05) of ESVs associated with anastomotic leak (non-AL or AL) in the preoperative gut microbiota in FMT mice.

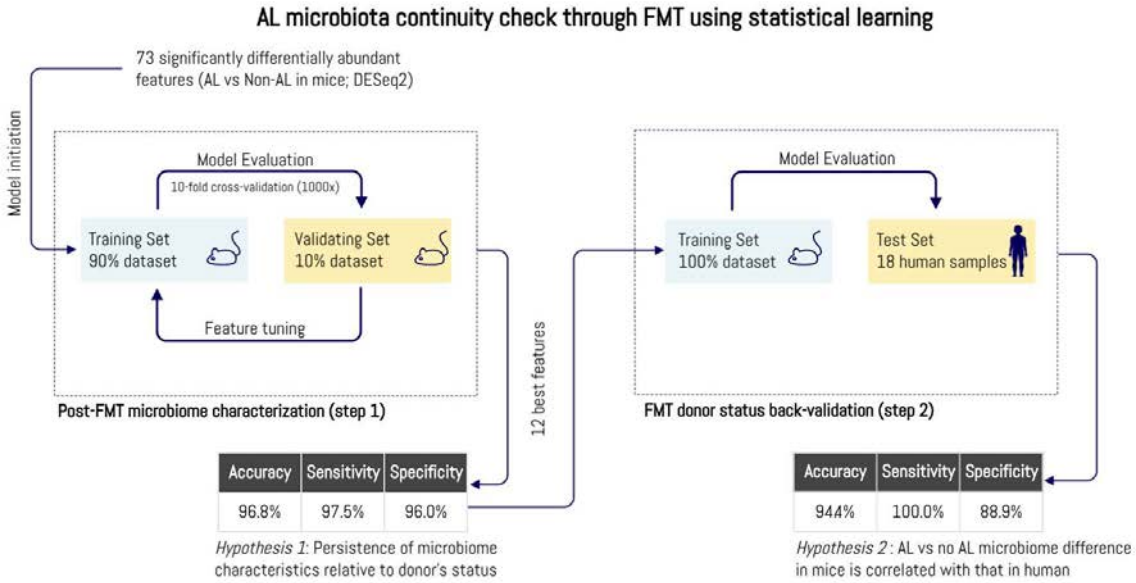

Supplementary figure 3. Gut microbiota features are associated with anastomotic leak (AL) in donors and FMT mice. To estimate whether mice could be accurately separated into non-AL and AL groups based solely on their microbiome characteristics (post-FMT microbiome characterization step), a logistic regression model was built using DESeq2 differentially abundant ESVs between post-FMT non-AL versus AL mice; uncharacterized sequences flagged as chimera were discarded). Feature (ESVs) tuning was achieved based on multiple iterative processes using 90% of the mice dataset as train set and the remaining 10% samples as a validation set. Twelve ESVs were selected as best features with a validation set prediction of 97.3% accuracy, 95.8% sensitivity, and 98.8% specificity. Secondly, to test whether the mice dataset best features can restore diagnosis in humans (FMT donor back-validation step), a second logistic regression model was trained on the full mice dataset (train set) using the previous model of 12 best features, and the status of all 18 human samples (test set) was predicted with a 94.4% accuracy (100% sensitivity and 88.9% specificity). The 12 features are depicted in Figure 1J.

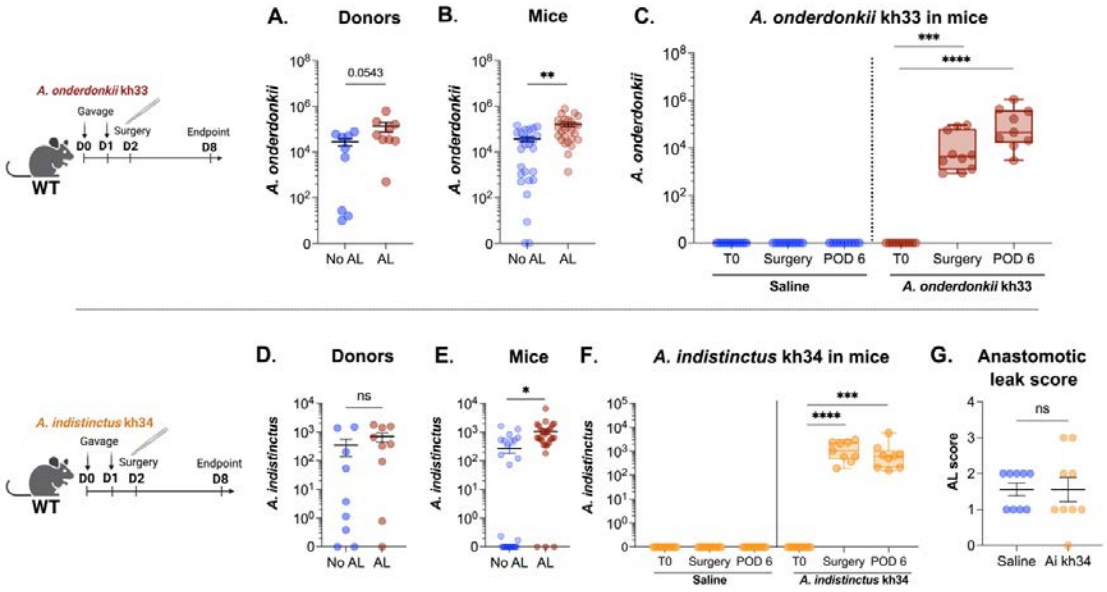

Supplementary figure 4. ***Alistipes onderdonkii*** **kh33, but not** ***Alistipes indistinctus*** **kh34, impairs colonic healing after surgery in mice**. (**A-F**) *A. onderdonkii* and *A. indistinctus*, quantified by qPCR in fecal samples of (**A and D**) donors without (No AL) and with anastomotic leak (AL). (**B and E**) mice after FMT from donors shown in A and D. Each symbol represents one donor or one mouse (27 mice per group; 3 mice per donor, 9 donors per group); bars are means ± SEM. *P* values were obtained using the generalized estimating equations (GEE) approach. (**C**, **F** and **G**) SPF wild-type mice received daily gavage with *A. onderdonkii* kh33, *A. indistinctus* kh34, or saline, before undergoing surgery. Fecal levels of (**C**) *A. onderdonkii* kh33 and (**F**) *A. indistinctus* kh34 in mice before (T0) and after bacterial supplementation. N=9 per group, each dot represents one mouse; Boxplots; Kruskal-Wallis test with Dunn's *post hoc* test. (**G**) Anastomotic leak (AL) score. N=9 per group. each dot represents one mouse with bars showing means ± SEM; two-tailed Student's *t*-test, **P*<0.05, ***P*<0.01, ****P*<0.001, *****P*<0.0001, ns, non-significant.

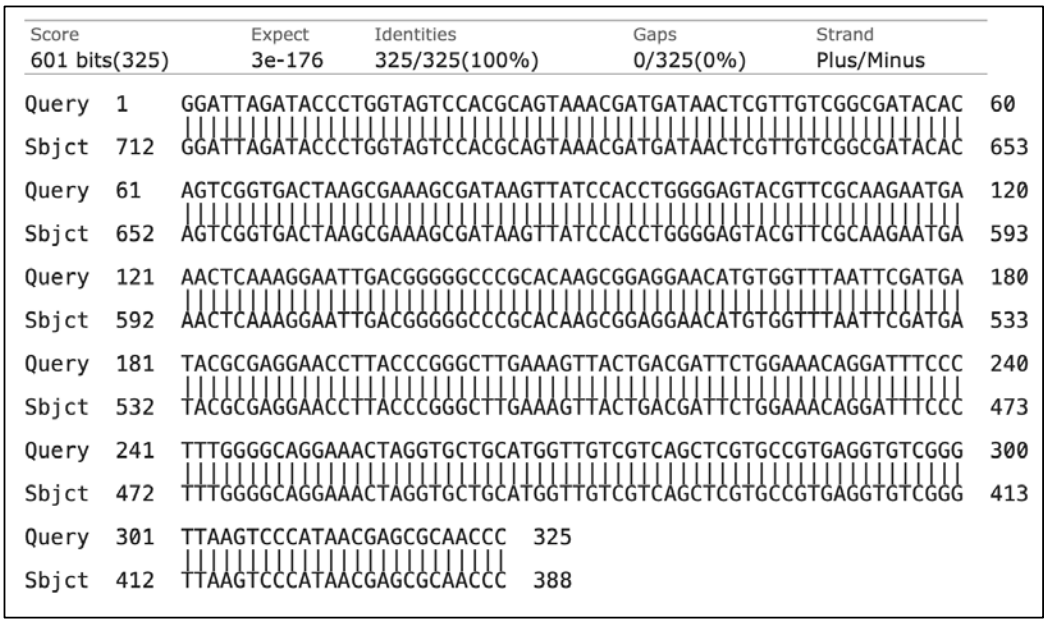

Supplementary figure 5. The variable V5-V6 region of a 16S rRNA gene of *Alistipes onderdonkii* kh33 is similar to *A. onderdonkii* ESV. Sequence alignment of *A. onderdonkii* and *A. onderdonkii* kh33 16S rRNA gene copy variant using NCBI BLASTn.

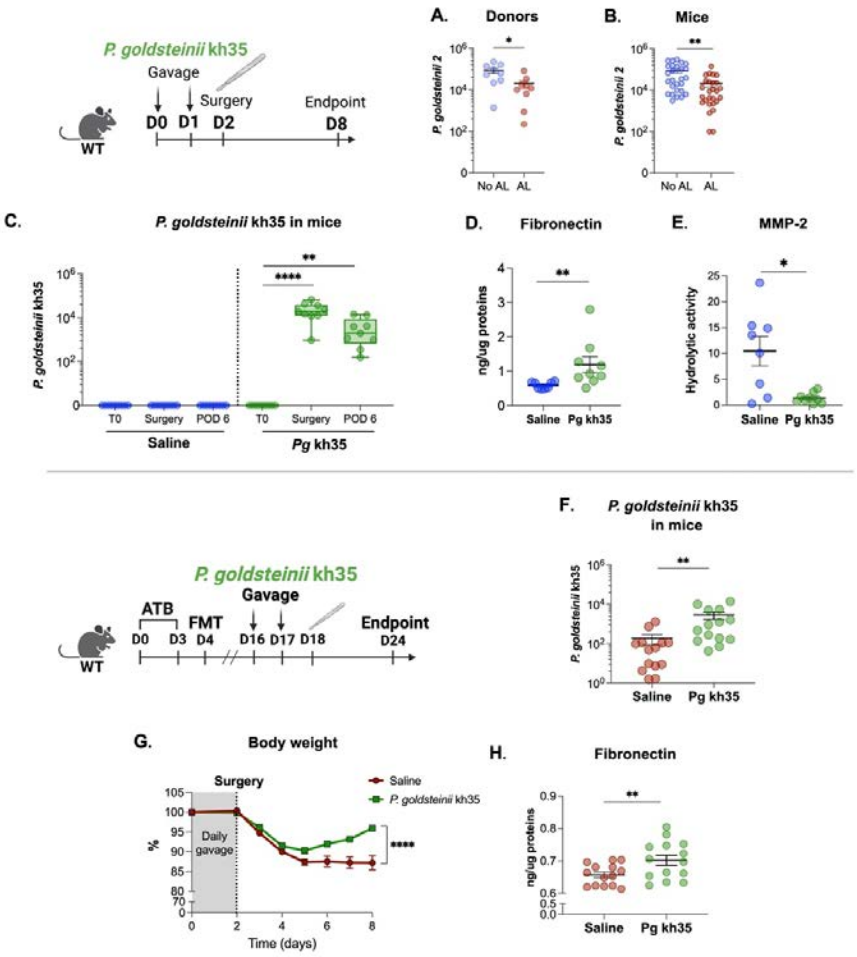

Supplementary figure 6. ***Parabacteroides goldsteinii* kh35 improves colonic surgical healing in mice**. **(A-B)** qPCR validation of *P. goldsteinii 2* ESV levels in (**A**) fecal samples of donors without anastomotic leak (No AL) and with anastomotic leak (AL), and in (**B**) mice after FMT from donors shown in A. Each symbol represents one donor or one mouse (27 mice per group; 3 mice per donor, 9 donors per group); bars are means ± SEM. *P* values were obtained using two-tailed *t*-test or the generalized estimating equations (GEE) approach. (**C-E**) SPF mice received saline or *P. goldsteinii* kh35 before undergoing colonic surgery. (**C**) Fecal levels of *P. goldsteinii* kh35, quantified by qPCR, in mice before (T0) and after bacterial supplementation. N=8-9 per group, each dot represents one mouse; Boxplots; Kruskal-Wallis test with Dunn's *post hoc* test. (**D**) Fibronectin concentration and (**E**) MMP-2 activity at the anastomotic wound. N = 8-9 mice per group; each dot represents one mouse with bars showing means ± SEM; two-tailed Student's *t*-test. (**F-J**) Antibiotic (ATB)-conditioned mice received FMT from CRC patients with AL and *P. goldsteinii* kh35 supplementation before undergoing colonic surgery. (**F**) Fecal levels of *P. goldsteinii* kh35 before surgery quantified by qPCR. (**G**) Body weight, (**H**) Fibronectin. N = 14 mice per group (2-3 mice per donor; 5 donors per group); *P* values were obtained using GEE. Data are represented as means ± SEM. **P*<0.05, ***P*<0.01, *****P*<0.0001.

A. Sequence alignment of *Parabacteroides goldsteinii* 1 and kh35

Score	Expect	Identities	Gaps	Strand
525 bits(284)	3e-153	313/327(96%)	2/327(0%)	Plus/Plus

```
Query  693  GGATTAGATACCCTGGTAGTCCACGCAGTAAACGATGATTACTAGCTGTTTGCGATACAC  752
            ||||||||||||||||||||||||||||||||||||||||||||||||||||||||||||
Sbjct  1    GGATTAGATACCCTGGTAGTCCACGCAGTAAACGATGATTACTAGCTGTTTGCGATACAC  60

Query  753  AGTAAGCGGCACAGCGAAAGCGTTAAGTAATCCACCTGGGGAGTACGCCGGCAACGGTGA  812
            ||||||||||||||||||||||||||||||||||||||||||||||||||||||||||||
Sbjct  61   AGTAAGCGGCACAGCGAAAGCGTTAAGTAATCCACCTGGGGAGTACGCCGGCAACGGTGA  120

Query  813  AACTCAAAGGAATTGACGGGGGCCCGCACAAGCGGAGGAACATGTGGTTTAATTCGATGA  872
            ||||||||||||||||||||||||||||||||||||||||||||||||||||||||||||
Sbjct  121  AACTCAAAGGAATTGACGGGGGCCCGCACAAGCGGAGGAACATGTGGTTTAATTCGATGA  180

Query  873  TACGCGAGGAACCTTACCCGGGTTTGAACGCATTCGGACCGGAGTGGAAACACT-TCTTC  931
            |||||||||||||||||||||||||||||||| |||| |||||||||||||| | |||
Sbjct  181  TACGCGAGGAACCTTACCCGGGTTTGAACGCATATTGACACCTCTGGAAACAGAGTC-TC  239

Query  932  TAGCAATAGCCGTTTGCGAGGTGCTGCATGGTTGTCGTCAGCTCGTGCCGTGAGGTGTCG  991
            |||||||||||||||||||||||||||||||||||||||||||||||||||||||||||||
Sbjct  240  TAGTAATAGCAATTTGCGAGGTGCTGCATGGTTGTCGTCAGCTCGTGCCGTGAGGTGTCG  299

Query  992  GCTTAAGTGCCATAACGAGCGCAACCC  1018
            |||||||||||||||||||||||||||
Sbjct  300  GCTTAAGTGCCATAACGAGCGCAACCC  326
```

B. Sequence alignment of *Parabacteroides goldsteinii 2* and kh35

Score	Expect	Identities	Gaps	Strand
603 bits(326)	1e-176	326/326(100%)	0/326(0%)	Plus/Plus

```
Query  693  GGATTAGATACCCTGGTAGTCCACGCAGTAAACGATGATTACTAGCTGTTTGCGATACAC  752
            ||||||||||||||||||||||||||||||||||||||||||||||||||||||||||||
Sbjct  1    GGATTAGATACCCTGGTAGTCCACGCAGTAAACGATGATTACTAGCTGTTTGCGATACAC  60

Query  753  AGTAAGCGGCACAGCGAAAGCGTTAAGTAATCCACCTGGGGAGTACGCCGGCAACGGTGA  812
            ||||||||||||||||||||||||||||||||||||||||||||||||||||||||||||
Sbjct  61   AGTAAGCGGCACAGCGAAAGCGTTAAGTAATCCACCTGGGGAGTACGCCGGCAACGGTGA  120

Query  813  AACTCAAAGGAATTGACGGGGGCCCGCACAAGCGGAGGAACATGTGGTTTAATTCGATGA  872
            ||||||||||||||||||||||||||||||||||||||||||||||||||||||||||||
Sbjct  121  AACTCAAAGGAATTGACGGGGGCCCGCACAAGCGGAGGAACATGTGGTTTAATTCGATGA  180

Query  873  TACGCGAGGAACCTTACCCGGGTTTGAACGCATTCGGACCGGAGTGGAAACACTTCTTCT  932
            ||||||||||||||||||||||||||||||||||||||||||||||||||||||||||||
Sbjct  181  TACGCGAGGAACCTTACCCGGGTTTGAACGCATTCGGACCGGAGTGGAAACACTTCTTCT  240

Query  933  AGCAATAGCCGTTTGCGAGGTGCTGCATGGTTGTCGTCAGCTCGTGCCGTGAGGTGTCGG  992
            ||||||||||||||||||||||||||||||||||||||||||||||||||||||||||||
Sbjct  241  AGCAATAGCCGTTTGCGAGGTGCTGCATGGTTGTCGTCAGCTCGTGCCGTGAGGTGTCGG  300

Query  993  CTTAAGTGCCATAACGAGCGCAACCC  1018
            ||||||||||||||||||||||||||
Sbjct  301  CTTAAGTGCCATAACGAGCGCAACCC  326
```

Supplementary figure 7. The variable V5-V6 region of a 16S rRNA gene of *Parabacteroides goldsteinii* kh35 is similar to *P. goldsteinii* 2 ESV. (**A**) Sequence alignment of *P. goldsteinii* 1 and (**B**) *P. goldsteinii* 2 ESV with *P. goldsteinii* kh35 16S rRNA gene copy variant using NCBI BLASTn. Red squares indicate mismatched nucleotides.

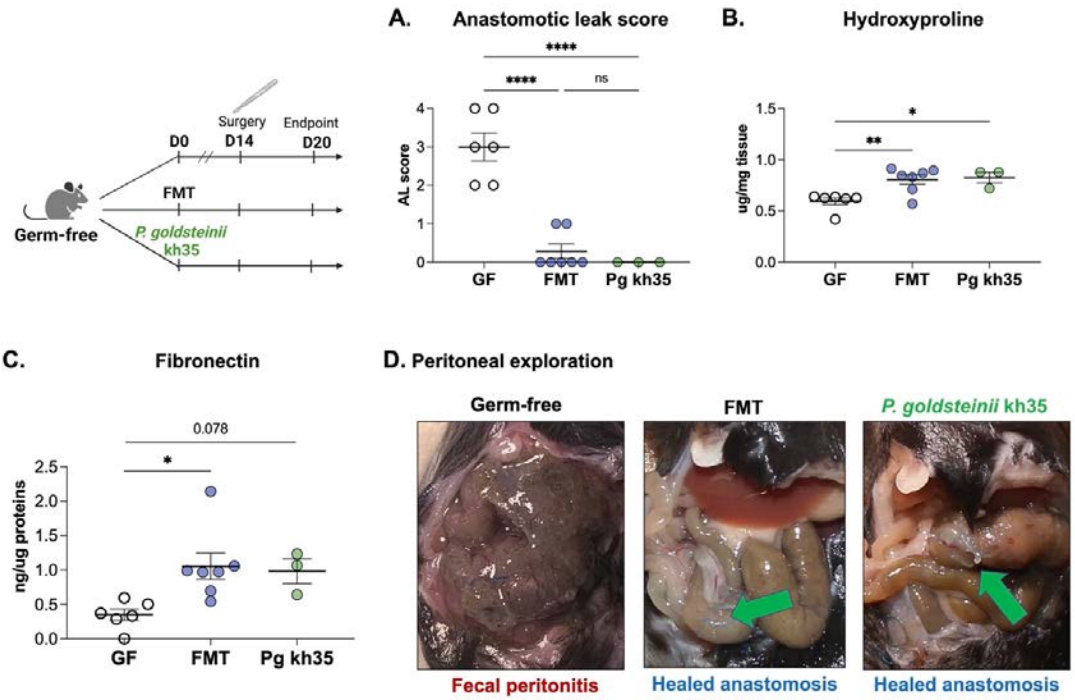

Supplementary figure 8. ***Parabacteroides goldsteinii*** **kh35 improves anastomotic healing in germ-free mice**. (**A-D**) Germ-free mice were gavaged with *P. goldsteinii* kh35 or with a pooled fecal sample from 4 healthy donors and were subjected to colonic surgery after 2 weeks. (**A**) Anastomotic leak (AL) score. (**B**) hydroxyproline and (**C**) fibronectin concentration at the anastomotic wound. N = 3-7 mice per group; each dot represents one mouse with bars showing means ± SEM; ANOVA with Tukey's *post hoc* test or Kruskal-Wallis test with Dunn's *post hoc* test, **P*<0.05, ***P*<0.01, *****P*<0.0001, ns, non-significant. (**D**) Representative picture of anastomotic healing in mice shows overt leak with peritonitis in a germ-free mouse (left), and healed anastomoses in mice colonized with the microbiota of healthy donors (middle) or with *P. goldsteinii* kh35 (right). Green arrows indicate the site of the anastomosis.

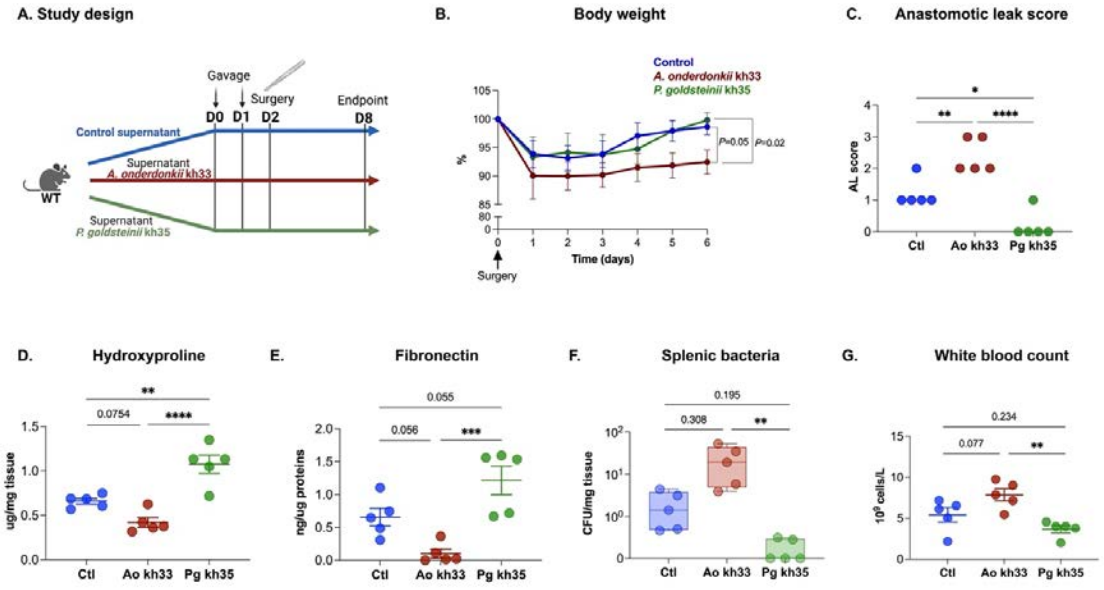

Supplementary figure 9. Secreted factors by *Alistipes onderdonkii* kh33 and *Parabacteroides goldsteinii* kh35 affect surgical colonic healing in mice. (**A**) SPF mice were gavaged on two consecutive days before surgery with supernatant from *Alistipes onderdonkii* kh33 (Ao kh33) or *P. goldsteinii* kh35 (Pg kh35) cultures, or with control supernatant from sterile medium. (**B**) Body weight of mice after surgery. (**C**) Anastomotic leak (AL) score, (**D**) hydroxyproline and (**E**) fibronectin at the anastomotic wound. N=5 mice per group, each dot represents one mouse with bars showing means ± SEM, ANOVA with Tukey's *post hoc* test. (**F**) Splenic bacteria. Boxplots, Kruskal-Wallis test with Dunn's *post hoc* test. (**G**) White blood cell count. Data are presented as means ± SEM, ANOVA with Tukey's *post hoc* test. **P*<0.05, ***P*<0.01, ****P*<0.001, *****P*<0.0001.

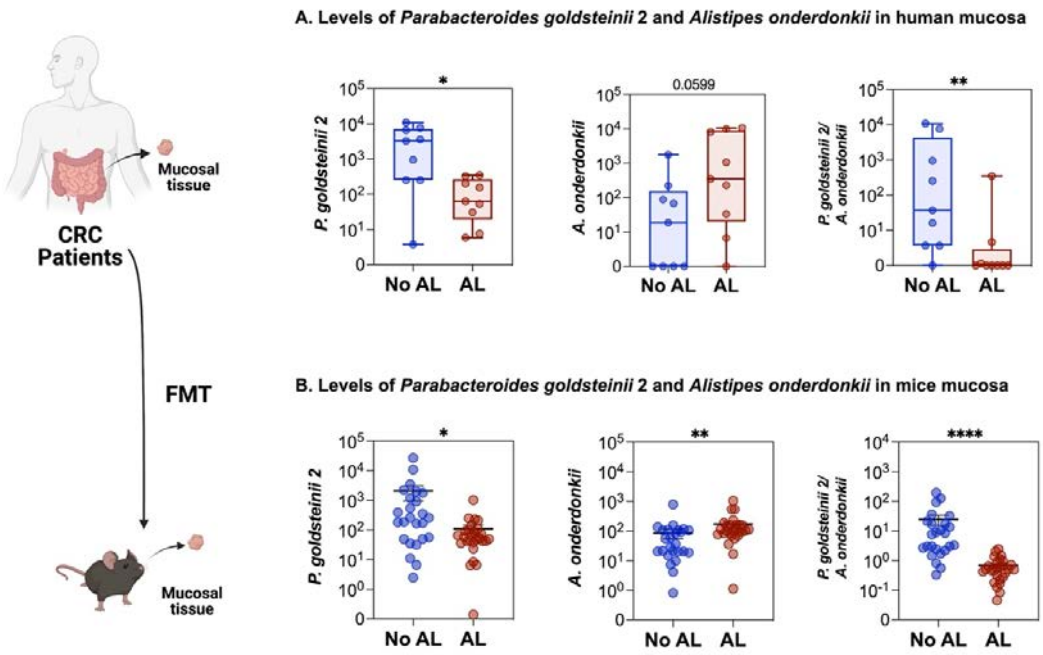

Supplementary figure 10. ***Alistipes onderdonkii*** **kh33 and** ***Parabacteroides goldsteinii*** **kh35 are present in the colonic mucosa and their levels are associated with postoperative anastomotic healing**. (**A-B**) *A. onderdonkii* and *P. goldsteinii* 2, assessed by quantitative PCR, and the ratio of *P. goldsteinii* 2 to *A. onderdonkii* in (**A**) mucosal biopsies collected during surgery. N=9 per group; Mann-Whitney U test; data are represented as boxplots and (**B**) in mucosal tissue collected from mice that received FMT from CRC patients without and with anastomotic leak (No AL and AL). N = 25-27 mice per group; 2-3 mice per donor; 9 donors per group; Bars are means ± SEM, GEE. **P*<0.05, ***P*<0.01, *****P*<0.0001.

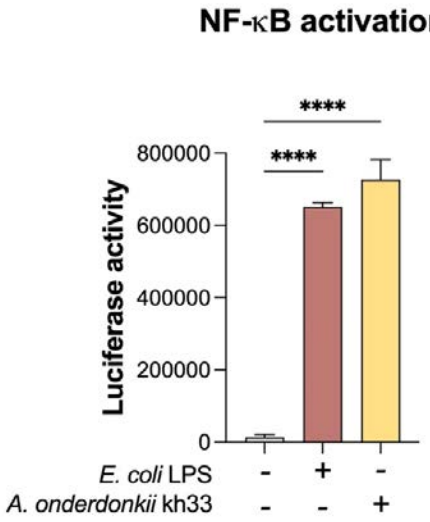

Supplementary figure 11. *Alistipes onderdonkii* kh33 supernatant activates the NF-κB signaling pathway in monocytic THP-1 cells. NF-κB activation (luciferase activity) by THP-1 cells treated with *Escherichia coli* LPS or with *A. onderdonkii* kh33 supernatant. N = 4 experiments; bars represent means ± SEM; ANOVA with Tukey's *post hoc* test. ****P<0.0001.

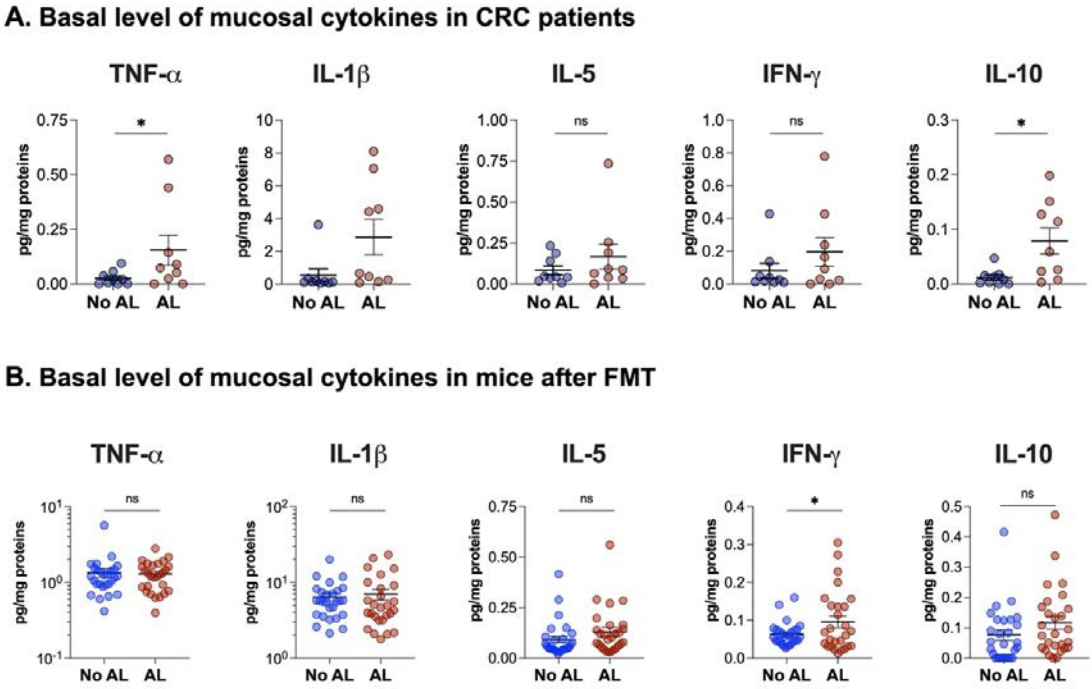

Supplementary figure 12. Basal levels of mucosal colonic cytokines in CRC patients. (**A**) The level of the following mucosal cytokines was assessed in CRC patients using a human cytokine multiplex assay: TNF-α, IL-1β, IL-17A/F, IL-5, IFN-γ and IL-10. N=9 donors per group, each dot represents one donor with bars showing means ± SEM, Two-tailed Student's *t*-test. (**B**) The level of the same mucosal cytokines was assessed in mice receiving FMT from donors shown in A using a mouse cytokine multiplex assay. Each symbol represents one mouse for a total of 54 mice (27/group; 3 mice per donor, 9 donors per group); Bars are means ± SEM, GEE. **P*<0.05; ns, non-significant.

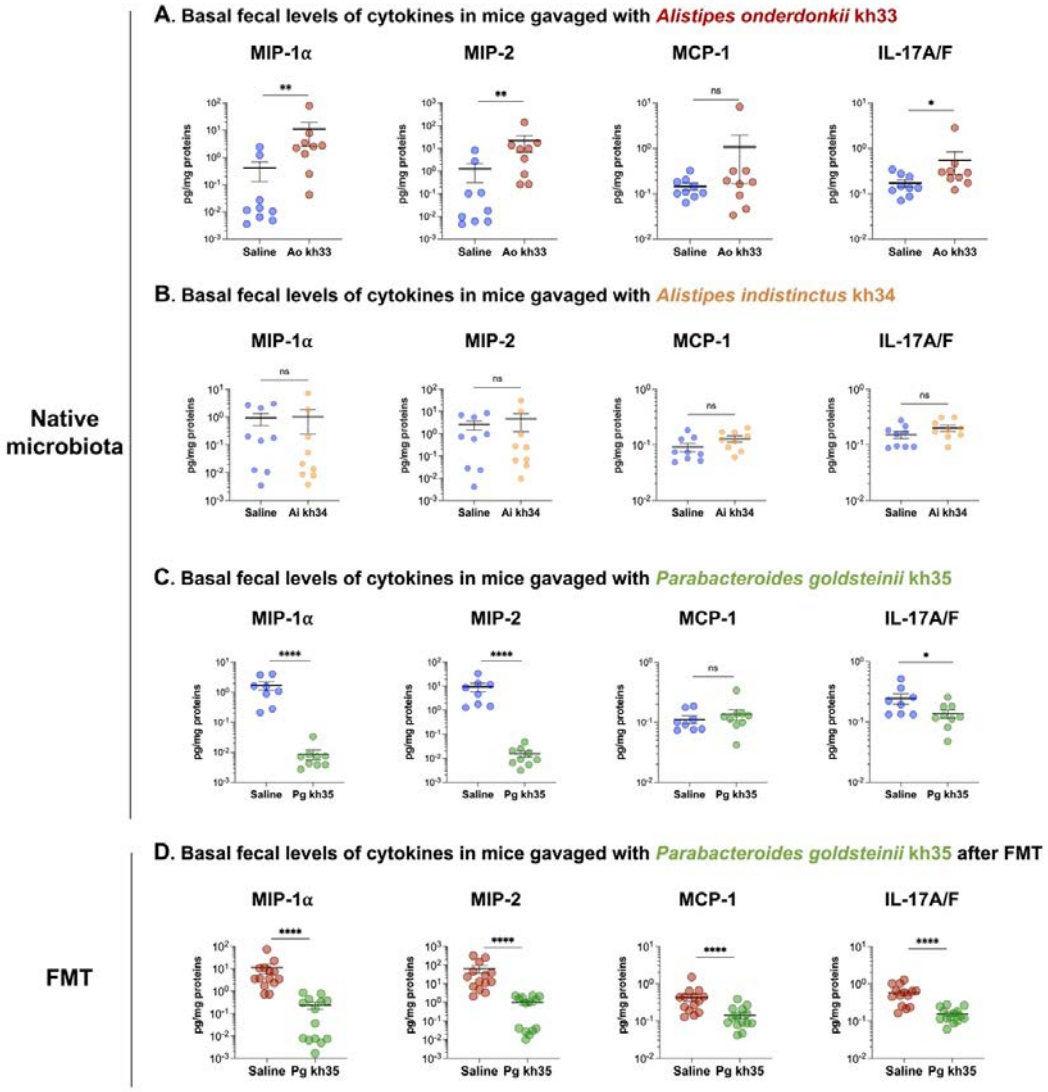

Supplementary figure 13. ***Alistipes onderdonkii*** **kh33 and** ***Parabacteroides goldsteinii*** **kh35 modulate the levels of intestinal inflammatory cytokines in mice. (A-C)** Fecal levels before surgery of interleukin 17A/F (IL-17A/F), macrophage inflammatory protein 1 alpha and 2 (MIP-1α and MIP-2) and monocyte chemoattractant protein 1 (MCP-1) in SPF mice after gavage with saline or (**A**) *A. onderdonkii* kh33, (**B**) *Alistipes indistinctus* kh34, and (**C**) *P. goldsteinii* kh35. N = 8-9 mice per group; each dot represents one mouse with bars showing means ± SEM; two-tailed Student's *t*-test. (**D**) Fecal levels before surgery of IL-17A/F, MIP-1α, MCP-1 and MIP-2 in antibiotic-conditioned mice that received FMT from CRC patients with AL, followed by oral gavage with saline or *P. goldsteinii* kh35. N = 14 mice per group (2-3 mice per donor; 5 donors per group); *P* values were obtained using GEE. Data are represented as means ± SEM. **P*<0.05, ***P*<0.01, *****P*<0.0001, ns, nonsignificant.

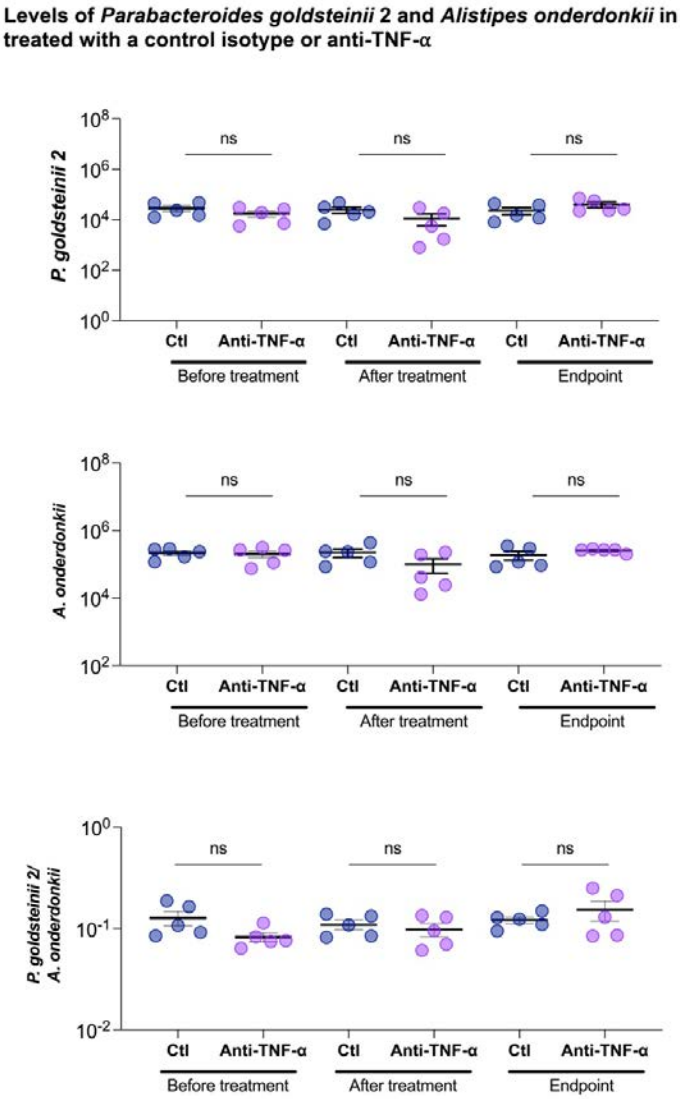

Supplementary figure 14. Fecal levels of *Parabacteroides goldsteinii* and *Alistipes onderdonkii* are not influenced by TNF-α blockade. *P. goldsteinii and A. onderdonkii*, assessed by quantitative PCR in fecal samples of mice before treatment with anti-TNF-α or a control isotype, after treatment but before surgery, and at endpoint. N=5 mice per group, each dot represents one mouse with bars showing means ± SEM, two-tailed Student's *t*-test; ns, non-significant.

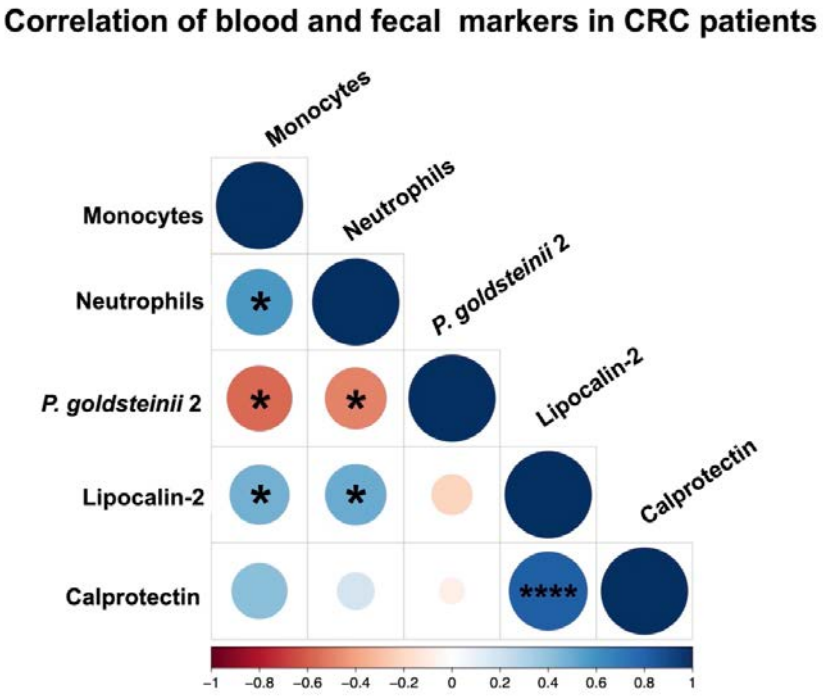

Supplementary figure 15. Correlation of blood monocyte and neutrophil counts and fecal *Parabacteroides goldsteinii* (qPCR), lipocalin-2 (ELISA) and calprotectin (ELISA) in CRC patients. Spearman correlation matrix. N=18. **P*<0.05, *****P*<0.0001.

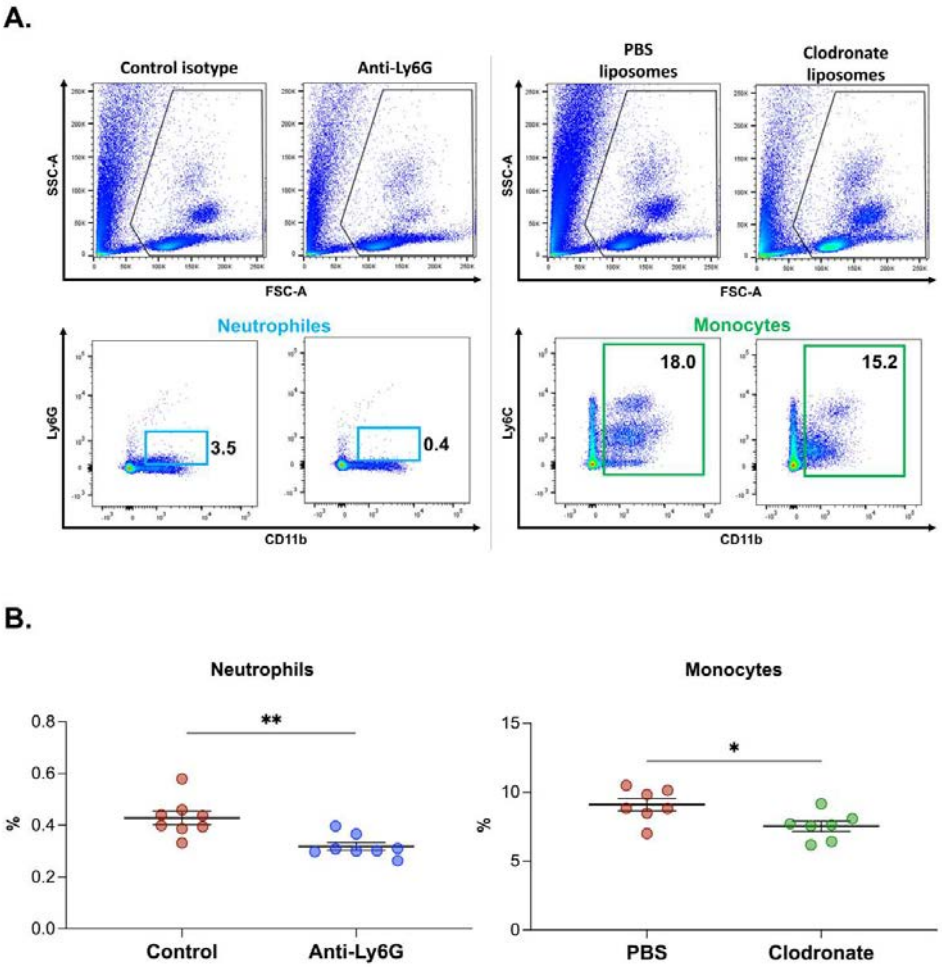

Supplementary figure 16. Neutrophil and monocyte depletion in mice. (**A**) Flow cytometry gating strategy to evaluate the depletion of monocytes and neutrophils in mice. Leukocytes were selected based on forward scatter, doublets were excluded and living cells were selected using a viability dye (not shown). Neutrophils were gated using $CD11b^{+}/Ly6G^{+}$ whereas $CD11b^{+}/Ly6C^{+}$ markers were used for gating monocytes. Representative charts of one mouse per group (**B**) Levels of neutrophils (%) and monocytes (%) in the blood in mice depleted with anti-Ly6G antibody and clodronate liposomes. N=7-8 mice per group, two-tailed Student's *t*-test, **P*<0.05, ***P*<0.01. Bars represent means ± SEM.

Supplementary table 1. Demographic, clinical, and perioperative data of patients and healthy donors.

CRC patients						
Age (years)	**Sex**	**Cancer location**	**Stage**	**Operation**	**AL**	**AL grade**
78	Male	Rectum	3	TATME	No	NA
39	Female	Rectum	3	LAR	No	NA
62	Male	Transverse colon	2	Left hemicolectomy	No	NA
76	Female	Sigmoid colon	3	LAR	No	NA
61	Male	Rectum	2	LAR	No	NA
52	Male	Rectum	2	LAR	No	NA
79	Male	Rectum	1	LAR	No	NA
70	Male	Rectum	2	LAR	No	NA
72	Male	Rectum	3	LAR	No	NA
71	Male	Rectum	3	LAR	Yes	C
63	Male	Rectum	1	LAR	Yes	B
77	Male	Rectum	2	TATME	Yes	B
75	Female	Transverse colon	1	Subtotal colectomy	Yes	B
52	Male	Sigmoid colon	1	LAR	Yes	C
76	Male	Rectum	2	LAR	Yes	C
65	Male	Rectum	3	LAR	Yes	C
55	Male	Sigmoid colon	2	LAR	Yes	B
43	Female	Rectum	3	LAR	Yes	C
Healthy donors						
58	Male	NA	NA	NA	NA	NA
50	Female	NA	NA	NA	NA	NA
59	Male	NA	NA	NA	NA	NA
55	Female	NA	NA	NA	NA	NA

AL, anastomotic leak; TATME, transanal total mesorectal excision; LAR, low anterior resection; NA, not applicable.

Supplementary table 2. Comparison of alpha-diversity indexes in donors and mice

Alpha-diversity index	Test	*P-value*	*P-adjusted*	FDR	Stat	intConf1	intConf2
No AL versus AL donors							
Chao1	*T*-test	0,5601	0,9802	0,6001	-0,6	-64	36
Evenness	Mann–Whitney	0,6665	NA	NA	-0,015	-0,1	0,073
InvSimpson	Mann–Whitney	1	NA	NA	-0,6	-13	15
Observed	*T*-test	0,3402	0,8611	0,5057	-0,98	-65	24
Shannon	Mann–Whitney	0,7304	NA	NA	-0,087	-0,58	0,48
Simpson	Mann–Whitney	1	NA	NA	-0,00085	-0,028	0,044
Mice before surgery receiving FMT from donors without and with AL							
Chao1	*T*-test	0,1969	0,8784	0,2954	-1,3	-32	6,7
Evenness	Mann–Whitney	0,0664	0,996	0,8424	0,026	-0,0032	0,056
InvSimpson	Mann–Whitney	0,07179	1	0,5205	2,9	-0,25	5,9
Observed	*T*-test	0,2433	0,8766	0,4562	-1,2	-31	8,1
Shannon	Mann–Whitney	0,2706	1	0,7066	0,12	-0,1	0,32
Simpson	Mann–Whitney	0,07179	1	0,5205	0,014	-0,00094	0,035
Mice after surgery receiving FMT from donors without and with AL							
Chao1	*T*-test	0,1638	0,6513	0,2769	-1,4	-43	7,4
Evenness	Mann–Whitney	0,611	NA	NA	-0,0082	-0,045	0,026
InvSimpson	Mann–Whitney	0,3533	NA	NA	-2,3	-6,7	2,6
Observed	*T*-test	0,1845	0,7566	0,3954	-1,3	-36	7,1
Shannon	Mann–Whitney	0,5012	NA	NA	-0,085	-0,31	0,16
Simpson	Mann–Whitney	0,3533	NA	NA	-0,0093	-0,03	0,0093

AL, anastomotic leak; NA, not applicable.

Supplementary table 3. Primers for real-time PCR

Target	Sequence (5'-3')		Amplicon size (bp)	Reference
16S rRNA gene*	Forward	CCATGAAGTCGGAATCGCTAG	86	*Eklöf et al.* (2017) (13)
	Reverse	GCTTGACGGGCGGTGT		
Alistipes indistinctus	Forward	GCACCGCATTGGTAAACTGG	210	This study
	Reverse	GTAATCGCTTGTGCCGTTCG		
Alistipes onderdonkii	Forward	AGAGGCATCTCTCCGGGTT	152	*Roager et al.* (2013) (14)
	Reverse	AGTCTGGTCCGTGTCTCAGT		
Parabacteroides goldsteinii 2	Forward	AAGCGTTAAGTAATCCACCTGG	149	This study
	Reverse	CCACTCCGGTCCGAATGC		
β-actin	Forward	AGAAAATCTGGCACCACACC	188	*Arthur et al.* (2017) (15)
	Reverse	AGAGGCGTACAGGGATAGCA		
TNF-α	Forward	TTGTTCCTCAGCCTCTTCTCCTCC	127	*Bergeron et al.* (2003) (16)
	Reverse	GAGGGCTGATTAGAGAGAGGT		

**16S* rRNA Gene Universal Bacteria Control Primers, NEBNext® Microbiome DNA Enrichment Kit (New England Biolabs Inc., Ipswich, MA, USA).

Supplementary table 4. Demographic and clinical data of CRC patients undergoing surgery between 2011 and 2021.

		No AL (N = 360)	**AL (N = 135)**
Age, median (range)		66 (22-94)	65 (25-88)
Sex	Female	158	36
	Male	202	99
CRC stage	1	71	27
	2	112	36
	3	134	46
	4	43	26
Operation	LAR	171	83
	Sigmoid colectomy	40	23
	Right hemicolectomy	93	13
	Subtotal colectomy	13	4
	Left hemicolectomy	18	4
	Extended right hemicolectomy	9	2
	Transverse colectomy	1	0
	Robotic LAR	8	2
	TaTME	5	3
	Proctectomy and right hemicolectomy/ileocolic resection	2	1

AL, anastomotic leak; CRC, colorectal cancer; LAR, low anterior resection; TaTME, Transanal total mesorectal excision

References

1. Hajjar R, Oliero M, Cuisiniere T, Fragoso G, Calve A, Djediai S*, et al.* Improvement of colonic healing and surgical recovery with perioperative supplementation of inulin and galacto-oligosaccharides. Clin Nutr **2021**;40(6):3842-51 doi 10.1016/j.clnu.2021.04.032.
2. Routy B, Le Chatelier E, Derosa L, Duong C, T. Alou M, Daillère R*, et al.* Gut microbiome influences efficacy of PD-1–based immunotherapy against epithelial tumors. Science **2018**;359:91-7.
3. Wiegerinck M, Hyoju SK, Mao J, Zaborin A, Adriaansens C, Salzman E*, et al.* Novel de novo synthesized phosphate carrier compound ABA-PEG20k-Pi20 suppresses collagenase production in Enterococcus faecalis and prevents colonic anastomotic leak in an experimental model. Br J Surg **2018**;105(10):1368-76 doi 10.1002/bjs.10859.
4. Hyoju SK, Klabbers RE, Aaron M, Krezalek MA, Zaborin A, Wiegerinck M*, et al.* Oral Polyphosphate Suppresses Bacterial Collagenase Production and Prevents Anastomotic Leak Due to Serratia marcescens and Pseudomonas aeruginosa. Ann Surg **2018**;267(6):1112-8 doi 10.1097/SLA.0000000000002167.
5. Kerem M, Bedirli A, Karahacioglu E, Pasaoglu H, Sahin O, Bayraktar N*, et al.* Effects of soluble fiber on matrix metalloproteinase-2 activity and healing of colon anastomosis in rats given radiotherapy. Clin Nutr **2006**;25(4):661-70 doi 10.1016/j.clnu.2006.01.028.
6. Collins TJ. ImageJ for microscopy. Biotechniques **2007**;43(1 Suppl):25-30 doi 10.2144/000112517.
7. Zhang Z, Schwartz S, Wagner L, Miller W. A greedy algorithm for aligning DNA sequences. J Comput Biol **2000**;7(1-2):203-14 doi 10.1089/10665270050081478.
8. Samba-Mondonga M, Constante M, Fragoso G, Calve A, Santos MM. Curcumin induces mild anemia in a DSS-induced colitis mouse model maintained on an iron-sufficient diet. PLoS One **2019**;14(4):e0208677 doi 10.1371/journal.pone.0208677.
9. McMurdie PJ, Holmes S. phyloseq: an R package for reproducible interactive analysis and graphics of microbiome census data. PLoS One **2013**;8(4):e61217 doi 10.1371/journal.pone.0061217.
10. Oksanen J BF, Friendly M, Kindt R, Legendre P, McGlinn D, Minchin PR, O'Hara RB, Simpson GL, Solymos P, Stevens MHH, Szoecs E, Wagner H (2020). vegan: Community Ecology Package.
11. Love MI, Huber W, Anders S. Moderated estimation of fold change and dispersion for RNA-seq data with DESeq2. Genome Biol **2014**;15(12):550 doi 10.1186/s13059-014-0550-8.
12. Fillebeen C, Gkouvatsos K, Fragoso G, Calve A, Garcia-Santos D, Buffler M*, et al.* Mice are poor heme absorbers and do not require intestinal Hmox1 for dietary heme iron assimilation. Haematologica **2015**;100(9):e334-7 doi 10.3324/haematol.2015.126870.
13. Eklof V, Lofgren-Burstrom A, Zingmark C, Edin S, Larsson P, Karling P*, et al.* Cancer-associated fecal microbial markers in colorectal cancer detection. Int J Cancer **2017**;141(12):2528-36 doi 10.1002/ijc.31011.
14. Roager HM, Licht TR, Poulsen SK, Larsen TM, Bahl MI. Microbial enterotypes, inferred by the prevotella-to-bacteroides ratio, remained stable during a 6-month randomized controlled diet intervention with the new nordic diet. Appl Environ Microbiol **2014**;80(3):1142-9 doi 10.1128/AEM.03549-13.

15. Arthur LL, Chung JJ, Jankirama P, Keefer KM, Kolotilin I, Pavlovic-Djuranovic S*, et al.* Rapid generation of hypomorphic mutations. Nat Commun **2017**;8:14112 doi 10.1038/ncomms14112.
16. Bergeron A, Soler P, Kambouchner M, Loiseau P, Milleron B, Valeyre D*, et al.* Cytokine profiles in idiopathic pulmonary fibrosis suggest an important role for TGF-beta and IL-10. Eur Respir J **2003**;22(1):69-76 doi 10.1183/09031936.03.00014703.